

Supporting Information

Self-Assembly of Fluorinated Sugar Amino Acid Derived α,γ -Cyclic Peptides into Transmembrane Anion Transport

Sachin S. Burade,[†] Tanmoy Saha,[‡] Naresh Bhuma,[†] Navanath Kumbhar,[†] Amol Kotmale,[§] Pattuparambil R. Rajamohanan,[§] Rajesh G. Gonnade,^{||} Pinaki Talukdar,^{*,‡} and Dilip D. Dhavale^{*,†}

[†]Garware Research Center, Department of Chemistry, Savitribai Phule Pune University (formerly Pune University), Pune 411007, India

[‡]Indian Institute of Science Education and Research (IISER), Pune 411008, India

[§]Central NMR Facility, ^{||}Center for Material Characterization (CMC), CSIR-NCL, Pune 411008, India

| Sr. No. | Table of Contents | Page Number |
|---------|---|-------------|
| 1. | General Methods | S2 |
| 2. | Experimental Procedure | S3 |
| 3. | Synthesis and characterization | S4 |
| 4. | Assignment of ¹ H-NMR data | S7 |
| 5. | IR spectra | S8 |
| 6. | ¹ H and ¹³ C NMR Spectra | S9 |
| 7. | 2D NMR Spectra | S17 |
| 8. | Schematic NOESY representation | S24 |
| 9. | HOESY spectra | S26 |
| 10. | Aggregation studies-concentration dependent NMR | S28 |
| 11. | Aggregation studies-ESI-MS | S29 |
| 12. | CD spectroscopy | S31 |
| 13. | Restrained Molecular Dynamics and Molecular modeling | S31 |
| 14. | X-ray Crystallography (CCDC 1573315) | S36 |
| 15. | Ion transport experiments | S37 |
| 16. | Anion recognition by ¹ H NMR titration | S42 |
| 17. | Anion recognition by ESI-MS spectroscopy | S42 |
| 18. | Geometry Optimization of [2 + NO ₃ ⁻] by DFT | S43 |
| 19. | References | S48 |

1. General Methods:

All reactions were carried out with distilled and dried solvents purchased from Sigma-Aldrich and Merk using oven-dried glassware. ^1H NMR (300 MHz/400 MHz/500 MHz) and ^{13}C NMR (75 MHz/100 MHz/125 MHz) and COSY, NOESY (500 MHz) and HOESY (500 MHz) were recorded in CDCl_3 on Bruker NMR instrument. The NMR spectras were processed using top-spin Bruker and MestreNova NMR softwares. Chemical shifts are reported in δ units (parts per million/ppm) with reference to TMS as an internal standard. Melting points was recorded using Thomas Hoover melting point apparatus and are uncorrected. Optical rotations were measured on a JASCO P-1020 a digital polarimeter with sodium light (589.3 nm) at 25 °C. High resolution mass spectra (HRMS) were recorded in positive as well as negative ion electron spray ionization (ESI) mode using a TOF (time of flight) analyzer. Thin layer chromatography was performed on pre-coated plates (0.25 mm, silica gel 60 F254, Merk). Column chromatography was carried out with silica gel (100–200 mesh). IR spectra were recorded on Shimadzu FT-IR spectrophotometer as a thin film or using KBr pellets in solid state and using IR solution cell in solution state and reported in cm^{-1} . The coupling reagents such as 1-[Bis(dimethylamino)methylene]-1*H*-1,2,3-triazolo[4,5-*b*]pyridinium 3-oxid hexafluorophosphate (HATU), 2-Chloro-1-methylpyridinium iodide (CMPI), Solvents like Diisopropylethylamine (DIPEA), Tetrahydrofuran (THF), Methanol (MeOH), acetonitrile were purchased from Sigma-Aldrich, which are used in solution phase peptide coupling reactions. After neutralization, workup involves washing of the combined organic layer with aqueous sodium bicarbonate, 1N HCl, water, brine, drying over anhydrous sodium sulfate and evaporation of solvent under reduced pressure. Circular dichroism (CD) was performed on JASCO J-1500 CD spectrometer using a cell of 2 mm path length. Spectra were recorded as an accumulation of 3 scans using a scan speed of 100nm/min, with resolution of 1.0 nm, band-width 5.0 nm and a response of 1 sec. Spectra were smoothened (5) and plotted using Origin Pro 6.0 software. Restraint molecular dynamics (MD) studies were carried out using the MacroModel with OPLS force field, version10.3 program from Schrodinger software. The constraints were derived from the volume integrals obtained from the NOESY spectra using a two-spin approximation and a reference distance of 1.8 Å for the geminal protons. The upper and lower bound of the distance constraints have been obtained by enhancing and reducing the derived distance by 10%. For ion transport study egg-yolk phosphatidylcholine (EYPC) and diphytanoylphosphatidylcholine (DPhPC) were obtained from Avanti Polar Lipids as a solution (25 mg/mL in CHCl_3) and solid respectively. 2-[4-(2-hydroxyethyl)piperazin-1-

yl]ethane sulfonic acid (HEPES) buffer, 8-hydroxypyrene-1,3,6-trisulfonate (HPTS) dye, lucigenin, Triton X-100, NaOH and inorganic salts were purchased of molecular biology grade from Sigma. The HEPES buffer solution was prepared in the Milli-Q water, which was collected from the filtration set up. The water was further autoclaved to get rid of microbial and related contaminations. The water was autoclaved prior to the buffer preparation because some buffers (e.g. HEPES) are not high temperature resistant. Dimethyl sulfoxide (DMSO) was purchased from Sigma-Aldrich. Fluorescence spectra were recorded from Fluoromax-4 from Jobin Yvon Edison equipped with an injector port and a magnetic stirrer. Measurements of pH were done using a Helmer pH meter. All data from fluorescence studies were processed either by KaleidaGraph 3.51 or Origin 8.5 program.

2. Experimental Procedure:

General Procedure for hydrolysis of methyl ester:

The methyl ester compound (1 equiv.) was dissolved in THF:MeOH:H₂O (3:1:1) mixture (100 mM). The solution was stirred at 0 °C for 5 min. LiOH (2.5 equiv.) was added slowly and the mixture was stirred vigorously at rt for 2 h. The solvent was concentrated under vacuo and diluted with water and acidified to approx. pH 4 with 2N HCl solution. The aqueous layer was extracted with ethyl acetate (Three times). The combined organic layer was dried over Na₂SO₄. The solvent was removed *in vacuo* to give the crude product. (For details, see individual procedures.)

General Procedure for conversion of azide to amine:

Azide compound (1 equiv.) was subjected for reduction in presence of H₂, 10% Pd/C (cat.) in methanol at rt for 2 h. Reaction mixture was filtered through celite bed. Organic solvent was concentrated under vacuum to give Product. (For details, see individual procedures).

General Procedure for Peptide coupling reaction:

To the stirred solution of amine compound (1 mmol), DIPEA (1 mmol) in dry CH₃CN under nitrogen atmosphere, acid compound (1 mmol) was added at 0 °C and stirred for 5 min; then HATU (1 mmol) was added at same temperature. After 5 min reaction was allowed to room temperature and continued for 12 h. Reaction mixture was diluted with EtOAc (100 mL) and the organic layer was washed with 1M HCl (50 mL) and saturated aqueous NaHCO₃ (50 mL) and brine. The organic layer was dried over Na₂SO₄. The solvent was removed *in vacuo* to give the crude product of peptide which was purified by column chromatography. (For details, see individual procedures).

General Procedure for Peptide macrocyclization via intramolecular coupling reaction:

Linear peptides (1mmol) were dissolved in THF:MeOH:H₂O (3:1:1) mixture (100 mM). The solution was stirred at 0 °C for 5 min. LiOH (2.5 equiv.) was added slowly and the mixture was stirred vigorously at rt for 2 h. The solvent was concentrated under vacuo and diluted with water and acidified to approx. pH 4 with 2N HCl solution. The aqueous layer was extracted with ethyl acetate (Three times). The combined organic layer was dried over Na₂SO₄. The solvent was removed *in vacuo* to give the crude product. This crude product containing azide was reduced in presence of H₂, 10% Pd/C (cat.) in methanol at rt for 2 h. Reaction mixture was filtered through celite bed. Organic solvent was concentrated under vacuum to give crude deprotected amine-acid terminal of peptide as crude material.

The crude amine-acid linear peptides **7** (1mmol) and **9** (1mmol) were dissolved in dry CH₃CN separately, with high dilution (~0.005 M) under inert atmosphere (Nitrogen gas), DIPEA (1mmol) and CMPI/HATU (1mmol) was added at rt. Reaction mixture was stirred for overnight at rt. Reaction mixture was diluted with EtOAc (50 mL) and the organic layer was washed with 1M HCl(aq) (25 mL) and saturated aqueous NaHCO₃ (25 mL) and brine. The organic layer was dried over Na₂SO_{4(s)}. The solvent was removed *in vacuo* to give the crude product of cyclic peptide which was purified by column chromatography. (For details, see individual procedures).

3. Synthesis and characterization:

(3S)-Carboxyloxy-[L-Val-OMe]-3-deoxy-3-fluoro-5-deoxy-5-amino-1,2-O-isopropylidene- α -D-xylo-1,4-furanose (**4**):

The compound **3**^[15] (2.5 g, 7.17 mmol) was subjected for reduction in presence of H₂, 10% Pd/C in methanol at rt for 2 h ($R_f = 0.3$, EtOAc:MeOH (9.5:0.5)). Reaction mixture was filtered through celite bed. Organic solvent was concentrated under vacuum to give thick liquid (2.1 g, 90% yield), $[\alpha]_D^{25} = -6.66$, ($c = 0.10$, MeOH), IR (neat): $\nu_{\max} = 3423.76$ (br), 3373.61 (br), 2966.62, 1741.78, 1685.84 cm⁻¹.

¹H NMR (300 MHz, CDCl₃): $\delta = 7.19$ (bd, $J = 7.8$ Hz, 1H, NH-val), 6.01 (d, $J = 3.8$ Hz, 1H, C1H), 4.70 – 4.58 (m, 3H, C2H, C4H & Val α H), 3.75 (s, 3H, OMe), 3.08 – 2.93 (m, 2H, C5H), 2.30 – 2.15 (m, 1H, Val β H), 1.91 (bs, 2H, exchangeable with D₂O, NH₂), 1.58 (s, 3H), 1.35 (s, 3H), 0.97 (d, $J = 6.8$, 3H), 0.94 (d, $J = 6.9$, 3H).

^{13}C NMR (125 MHz, CDCl_3): $\delta = 171.2, 164.9$ (d, $J = 21.9$ Hz), 113.8, 104.9, 100.6 (d, $J = 193.6$ Hz), 85.0 (d, $J = 37.2$ Hz), 82.7 (d, $J = 21.9$ Hz), 57.3, 52.4, 39.5 (d, $J = 7.8$ Hz), 31.2, 27.0, 26.7, 19.0, 17.9. HRMS (ESI-TOF) m/z : $[\text{M}+\text{H}]^+$ calcd for $\text{C}_{15}\text{H}_{26}\text{FN}_2\text{O}_6$, 349.1769, found 349.1764.

(3S)-Carbonyloxy-[L-Val-OH]-3-deoxy-3-fluoro-5-deoxy-5-azido-1,2-O-isopropylidene- α -D-xyllo-1,4-furanose (5):

Compound **3** (2.1 g, 5.61 mmol) was hydrolyzed using above general procedure for hydrolysis of methyl ester that afforded acid compound **5** as a white solid, 2 g, 95% yield, ($R_f = 0.5$, EtOAc) Mp = 135–137 °C, $[\alpha]_{\text{D}}^{25} = -17.33$ ($c = 0.11$, MeOH), IR (KBr): $\nu_{\text{max}} = 3399.5$ (br), 3390 – 2800, 2096.4 (N_3), 1724, 1691 cm^{-1} .

^1H NMR (500 MHz, CDCl_3): $\delta = 6.88$ (dd, $J = 8.8$ & 1.6 Hz, 1H, NH-val), 6.06 (d, $J = 3.9$ Hz, 1H, C1H), 4.85 – 4.76 (m, 1H, C4H), 4.67 (dd, $J = 14.8$ & 3.9 Hz, 1H, C2H), 4.60 (dd, $J = 8.3$ & 4.4 Hz, 1H, Val α H), 3.60 (dd, $J = 13.2$ & 6.7 Hz, 1H, C5H), 3.43 (dd, $J = 13.2$ & 5.2 Hz, 1H, C5H), 2.35 – 2.25 (m, 1H, Val β H), 1.58 (s, 3H, CH_3), 1.35 (s, 3H, CH_3), 1.03 (d, $J = 6.8$, 3H, CH_3), 0.99 (d, $J = 6.9$, 3H, CH_3).

^{13}C NMR (125 MHz, CDCl_3): $\delta = 175.6, 164.2$ (d, $J = 21.9$ Hz), 114.1, 105.2, 100.0 (d, $J = 195.3$ Hz), 84.6 (d, $J = 37.2$ Hz), 79.8 (d, $J = 19.5$ Hz), 57.0, 48.2 (d, $J = 8.0$ Hz), 30.9, 26.9, 26.5, 18.9, 17.56. HRMS (ESI-TOF) m/z : $[\text{M}+\text{Na}]^+$ calcd for $\text{C}_{14}\text{H}_{21}\text{FN}_4\text{O}_6$, 383.1337, found 383.1343.

Linear tetrapeptide (6):

Compound **4** (2 g, 5.55 mmol) and **5** (5.55 mmol) was coupled using above general procedure to get tetrapeptide ($R_f = 0.4$, EtOAc:Hexane (4:6) as white solid, 3.2 g, 83.5% yield, Mp = 77-79 °C, $[\alpha]_{\text{D}}^{25} = -34.83$ ($c = 0.1$, MeOH), IR (KBr): $\nu_{\text{max}} = 3330.1$ (br), 3360 – 2878 (br), 2103.8 (N_3), 1739.1, 1661.9, 1000 – 1111.2 (strong), 1160 – 1377 cm^{-1} .

^1H NMR (500 MHz, CDCl_3): $\delta = 7.06$ (dd, $J = 8.5$ & 1.2 Hz, 1H, NH-val), 6.92 (dd, $J = 8.3$ & 3.0 Hz, 1H, NH'-val), 6.39 (t, $J = 5.7$ Hz, 1H, C5NH), 6.03 (d, $J = 3.9$ Hz, 1H, C1H), 6.00 (d, $J = 3.8$ Hz, 1H, C1H'), 4.85 – 4.60 (m, 4H, C2 & C4H & C4H'), 4.55 (dd, $J = 8.5$ & 4.6 Hz, 1H, Val α H), 4.33 (dd, $J = 8.3$ & 6.09 Hz, 1H, Val α H'), 3.78 (s, 3H, OCH_3), 3.74 – 3.66 (m, 1H, C5H/H'), 3.61 – 3.50 (m, 2H, C5H/H'), 3.45 (dd, $J = 13.0$ & 4.8 Hz, 1H, C5H/H'), 2.30 – 2.20 (m, 1H, Val β H/H'), 2.14 – 2.04 (m, 1H, Val β H/H'), 1.55 (s, 3H, CH_3), 1.54 (s, 3H, CH_3), 1.33 (s, 6H, 2 x CH_3), 0.98 (d, $J = 6.9$, 3H, CH_3), 0.94 (d, $J = 6.9$, 6H, 2 x CH_3), 0.90 (d, $J = 6.8$ Hz, 3H, CH_3).

^{13}C NMR (125 MHz, CDCl_3): $\delta = 172.1, 170.5, 164.3$ (d, $J = 21.8$ Hz), 163.7 (d, $J = 22.0$ Hz), 114.0, 113.9, 105.2, 104.9, 98.8 (d, $J = 194.4$ Hz), 99.6 (d, $J = 193.7$ Hz), 84.7 (d, $J = 37.5$ Hz), 84.5 (d, $J = 37.3$ Hz), 79.8 (d, $J = 19.6$ Hz), 79.3 (d, $J = 19.5$ Hz), 57.9, 57.2, 52.6, 48.4 (d, $J = 8.2$ Hz), 36.5 (d, $J = 8.5$ Hz), 31.4, 30.8, 26.9 (s), 26.6, 26.5, 19.2, 19.0, 17.7, 17.6. HRMS (ESI-TOF) m/z : $[\text{M}+\text{Na}]^+$ calcd for $\text{C}_{29}\text{H}_{44}\text{F}_2\text{N}_6\text{O}_{11}$, 713.2928, found 713.2940.

Linear hexapeptide (8):

Compound **6** (2 g, 2.88 mmol) was dissolved in methanol in presence of 10% Pd/C under H₂ at balloon pressure to give amine (please see general procedure for reduction of azide to amine) compound (1 equiv.) that on coupling with **5** (1 equiv.) using above general procedure to get hexapeptide **8** (*R_f* = 0.6, EtOAc:Hexane (1:1) as white solid, 2.3 g, 78.8% yield (over 2 step), Mp = 104-106 °C, [α]_D²⁵ = -8.4 (*c* = 0.11, MeOH), IR (KBr): ν_{\max} = 3343.5, 2961 – 2875, 2106.9 (N₃), 1742.9, 1660.5, 1000 – 1146.4 (strong), 1200 – 1375 cm⁻¹.

¹H NMR (500 MHz, CDCl₃): δ = 7.10 (bt, *J* = 7.3 Hz, 2H, 2 x NH_{1,2}-val), 7.00 (dd, *J* = 8.4 & 2.8 Hz, 1H, NH₃-val), 6.74 – 6.68 (m, 1H, C₅NH₁), 6.67 – 6.60 (m, 1H, C₅NH₂), 6.05 (d, *J* = 3.8 Hz, 1H, C₁H₁), 6.02 (d, *J* = 3.7 Hz, 1H, C₁H₂), 6.00 (d, *J* = 3.8 Hz, 1H, C₁H₃), 4.83 – 4.60 (m, 6H, C₂- & C₄-H, 1,2,3), 4.53 (dd, *J* = 8.4 & 4.7 Hz, 1H, Val α H₁), 4.37 – 4.29 (m, 2H, 2 x Val α H), 3.80 (s, 3H, OCH₃), 3.80 – 3.44 (m, 6H, 3 x C₅CH₂), 2.30 – 2.20 (m, 1H, Val β H), 2.22 – 2.05 (m, 2H, 2 x Val β H), 1.55 (s, 3H, CH₃), 1.54 (s, 3H, CH₃), 1.35 (s, 3H, CH₃), 1.34 (s, 6H, 2 x CH₃), 0.97 (d, *J* = 6.9, 3H, CH₃), 0.93 – 0.91 (m, 9H, 3 x CH₃), 0.88 (d, *J* = 6.8 Hz, 3H, CH₃).

¹³C NMR (125 MHz, CDCl₃): δ = 172.1, 170.8, 170.5, 164.5 (d, *J* = 21.9 Hz), 164.2 (d, *J* = 21.9 Hz), 163.8 (d, *J* = 22.0 Hz), 114.0, 113.9, 113.8, 105.2, 104.9, 104.8, 100.2 (d, *J* = 194.8 Hz), 100.1 (d, *J* = 194.6 Hz), 100.0 (d, *J* = 194.7 Hz), 84.7 (d, *J* = 37.4 Hz), 84.5 (d, *J* = 37.6 Hz), 84.4 (d, *J* = 37.3 Hz), 79.9 (d, *J* = 19.6 Hz), 79.3 (d, *J* = 19.1 Hz), 79.1 (d, *J* = 17.9 Hz), 58.1, 58.0, 57.3, 52.6, 48.4 (d, *J* = 8.2 Hz), 36.8 (d, *J* = 9.0 Hz), 36.7 (d, *J* = 9.7 Hz), 31.2, 31.0, 30.8, 26.9, 26.8, 26.8, 26.6, 26.5 (s), 19.2, 19.1, 18.9, 17.7, 17.6, 17.5. HRMS (ESI-TOF) *m/z*: [M+Na]⁺ calcd for C₄₃H₆₅F₃N₈O₁₆, 1029.4363, found 1029.4358.

Cyclo-[(3*S*, 4*R*)- γ -FFSAA-(*S*)-Val-(3*S*, 4*R*)- γ -FFSAA-(*S*)-Val] (1):

Compound **6** (1 g, 1.44 mmol) was converted to compound **1** by using general procedure for macrocyclization. Compound **1** (*R_f* = 0.5, EtOAc:Hexane (6:4) as white solid, 0.55 g, 60% yield (over 2 step), Mp = 224 – 226 °C, IR (KBr): ν_{\max} = 3420.0 (br), 3382.6 (br), 3274.6, 1664.7, 1579.5, 1376.6 – 1221, 1164.3 – 979.7(strong).

¹H NMR (500 MHz, CDCl₃, 9.48 mM): δ = 7.13 (dd, *J* = 8.5 & 2.9 Hz, 2H, 2 x NH-val), 6.23 (d, *J* = 8.5 Hz, 2H, 2 x C₅NH), 6.00 (d, *J* = 3.9 Hz, 2H, 2 x C₁H), 4.87 (ddd, *J* = 25.7, 11.4 & 4.0 Hz, 2H, 2 x C₄H), 4.63 (dd, *J* = 14.5 & 3.9 Hz, 2H, 2 x C₂H), 4.26 – 4.14 (m, 4H, 2 x Val α H & 2 x C₅H₁), 3.20 (bd, *J* = 13.3 Hz, 2H, 2 x C₅H₂), 2.05 – 1.90 (m, 2H, 2 x Val β H), 1.52 (s, 6H, 2 x CH₃), 1.31 (s, 6H, 2 x CH₃), 0.92 (d, *J* = 7.0 Hz, 6H, 2 x CH₃Val), 0.90 (d, *J* = 6.9 Hz, 6H, 2 x CH₃Val).

¹³C NMR (125 MHz, CDCl₃): δ = 169.7, 164.1 (d, *J* = 21.4 Hz), 113.5, 104.9, 99.4 (d, *J* = 200 Hz), 85.3 (d, *J* = 37.9 Hz), 78.0 (d, *J* = 21.3 Hz), 57.1, 35.5 (d, *J* = 8.0 Hz), 32.9, 26.8, 26.7, 18.4, 18.3. HRMS (ESI-TOF) *m/z*: [M+H]⁺ calcd for C₂₈H₄₃F₂N₄O₁₀, 633.2942, found, 633.2948.

Cyclo-[(3*S*, 4*R*)- γ -FFSAA-(*S*)-Val-(3*S*, 4*R*)- γ -FFSAA-(*S*)-Val-(3*S*, 4*R*)- γ -FFSAA-(*S*)-Val]
(2):

Compound **8** (1 g, 0.99 mmol) was converted to compound **2** by using general procedure for macrocyclization. Compound **2** ($R_f = 0.6$, EtOAc:Hexane (8:2) as white solid, 0.5 g, 53% yield (over 2 step), Mp = 214 – 216 °C, IR (KBr): $\nu_{\max} = 3309.3$ (br), 1658.7, 1377.4, 1219.2, 1162 – 1031.6 (strong)

^1H NMR (500 MHz, CDCl_3 , 3 mM): $\delta = 7.03$ (dd, $J = 8.6$ & 2.2 Hz, 3H, 3 x NH-val), 6.72 (dd, $J = 6.6$ & 4.3 Hz, 3H, 3 x C5NH), 6.00 (d, $J = 3.8$ Hz, 3H, 3 x C1H), 4.69 (dd, $J = 13.8$ & 3.9 Hz, 3H, 3 x C2H), 4.60 (ddd, $J = 25.9$, 7.5 & 5.4 Hz, 3H, 3 x C4H), 4.47 (dd, $J = 8.6$ & 4.8 Hz, 3H, 3 x Val α H), 3.98 – 3.89 (m, 3H, C5H₁), 3.53 (ddd, $J = 13.8$, 7.6 & 4.2 Hz, 3H, 3 x C5H₂), 2.30 – 2.21 (m, 3H, 3 x Val β H), 1.58 (s, 9H, 3 x CH₃, merged with H₂O), 1.36 (s, 9H, 3 x CH₃), 0.94 (d, $J = 6.8$ Hz, 9H, 3 x CH₃), 0.88 (d, $J = 6.9$ Hz, 9H, 3 x CH₃).

^{13}C NMR (125 MHz, CDCl_3): $\delta = 170.3$, 164.6 (d, $J = 22.0$ Hz), 114.2, 104.8, 99.6 (d, $J = 194.3$ Hz), 84.6 (d, $J = 37.7$ Hz), 79.5 (d, $J = 19.9$ Hz), 58.0, 36.4 (d, $J = 8.4$ Hz), 30.6, 26.9, 26.6, 18.9, 17.6. HRMS (ESI-TOF) m/z : $[\text{M}+\text{Na}]^+$ calcd for $\text{C}_{42}\text{H}_{64}\text{F}_3\text{N}_6\text{O}_{15}$, 971.4196, found 971.4206.

4. Assignment of ^1H -NMR data:

Table S1: ^1H NMR (500 MHz, CDCl_3) data of **1** and **2**: Chemical shift (δ ppm), multiplicity, and Coupling constant (J in Hz)

| *Proton | 1 (60 mM) | 2 (50 mM) |
|---------------------|---|--|
| Val-NH | 7.21 (dd, $J = 8.94$ & 3.19 Hz) | 7.08 (dd, $J = 8.7$ & 2.2 Hz) |
| C5-NH | 6.75 (d, $J = 9.20$ Hz) | 6.78 (dd, $J = 6.6$ & 4.3 Hz) |
| C1H | 6.02 (d, $J = 3.9$ Hz) | 6.02 (d, $J = 3.8$ Hz) |
| C2H | 4.65 (dd, $J = 14.5$ & 3.9 Hz) | 4.71 (dd, $J = 13.8$ & 3.9 Hz) |
| C4H | 4.84 (ddd, $J = 25.7$, 11.4 & 4.0 Hz) | 4.60 (ddd, $J = 25.9$, 7.5 & 5.4 Hz) |
| C5Ha | 4.24 (m) | 3.98 - 3.89 (m, 3H) |
| C5Hb | 3.16 (bd, $J = 13.3$ Hz) | 3.53 (ddd, $J = 13.8$, 7.6 & 4.2 Hz) |
| Val- α H | 4.47 (dd, $J = 8.31$ & 7.32 Hz) | 4.47 (dd, $J = 8.6$ & 4.8 Hz) |
| Val- β H | 2.05 - 1.90 (m) | 2.30 - 2.21 (m) |
| Acetonide | 1.52 (s) & 1.31 (s) | 1.58 (s, merged with H ₂ O), 1.36 (s) |
| Val-CH ₃ | 0.92 (d, $J = 7.0$ Hz), 0.90 (d, $J = 6.9$ Hz) | 0.94 (d, $J = 6.8$ Hz), 0.88 (d, $J = 6.9$ Hz). |

* **1** showed each signal for 2 sets of proton and **2** showed each signal for 3 sets of proton

5. IR spectra:

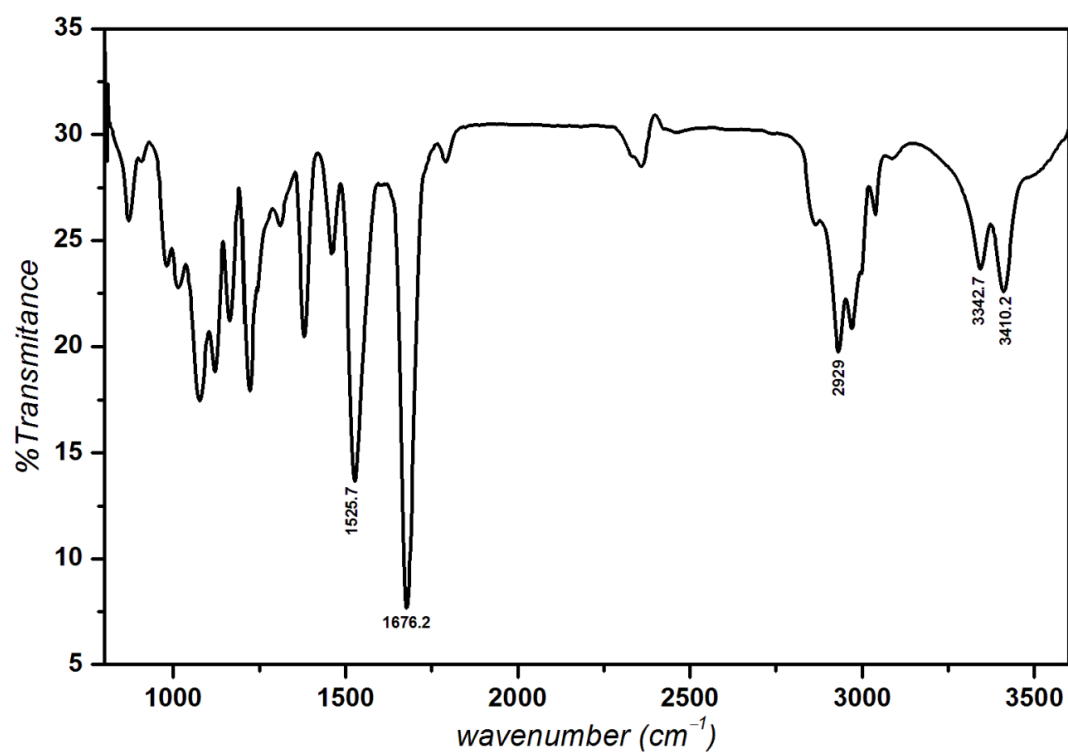


Figure S1: IR spectra of FCTP 1 at 20 mM concentration in CHCl₃ solution at 25 °C.

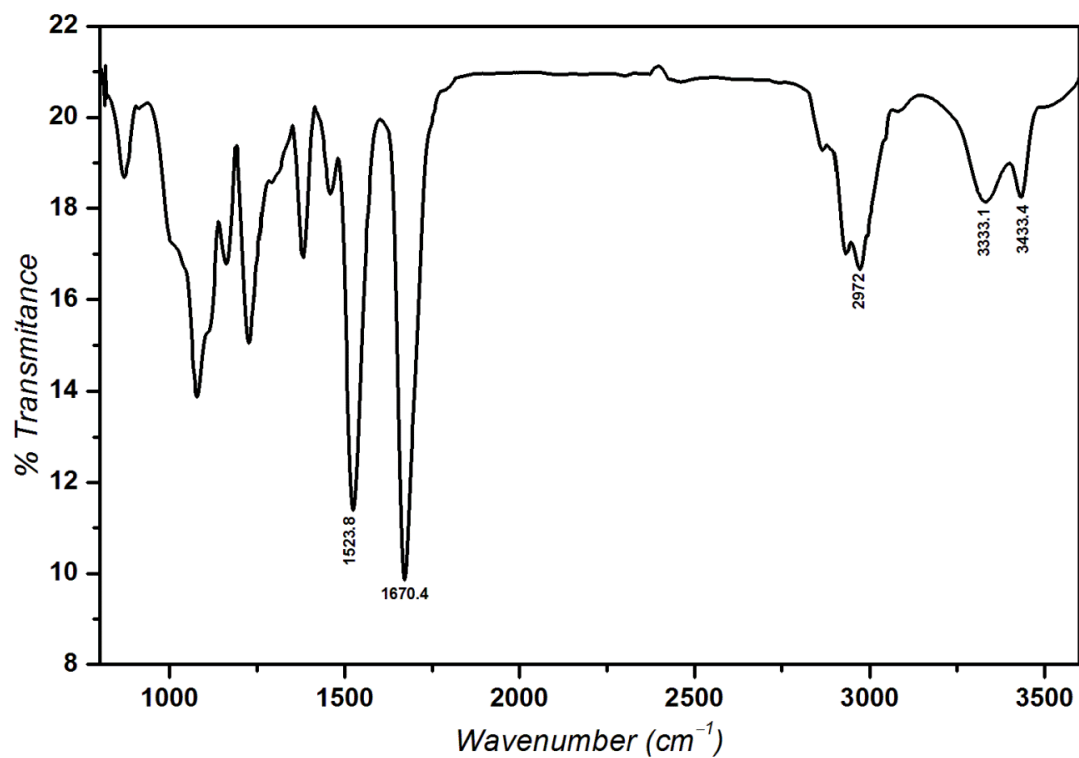


Figure S2: IR spectra of FCHP 2 at 20 mM concentration in CHCl₃ solution at 25 °C.

6. ^1H and ^{13}C NMR Spectra:

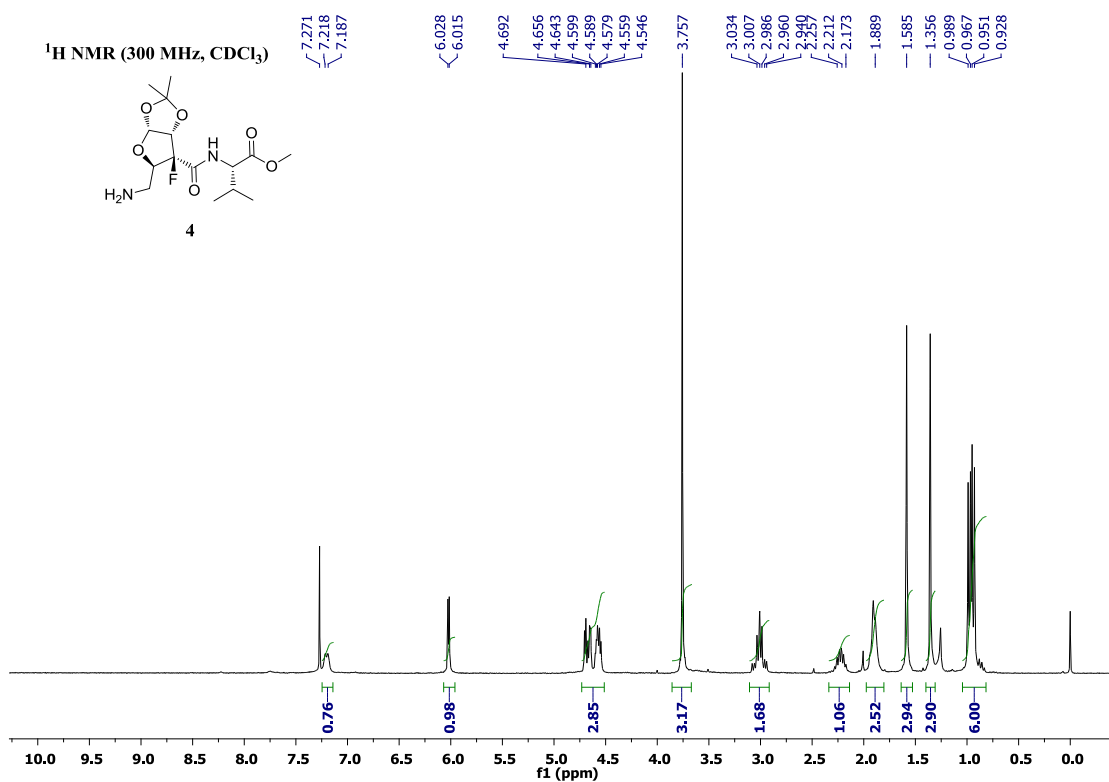


Figure S3: ^1H NMR spectra of compound **4** on 300 MHz in CDCl_3 .

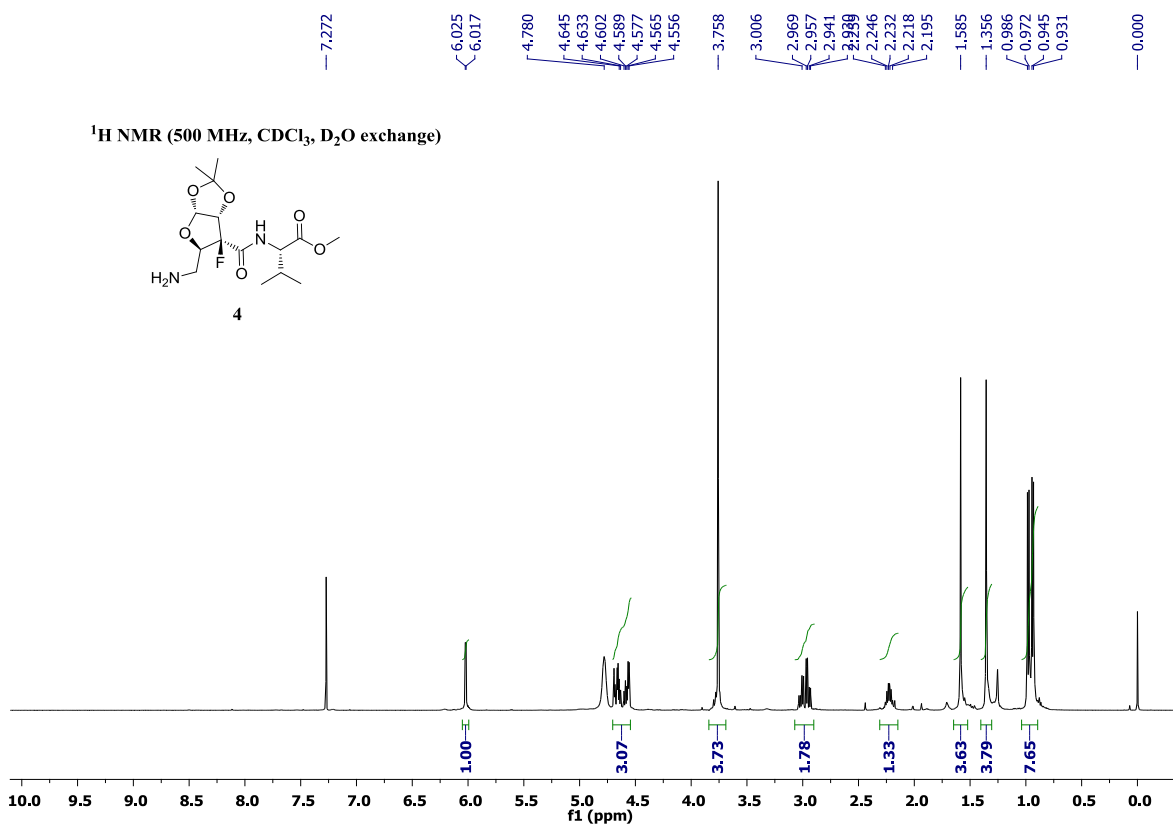


Figure S4: ^1H NMR spectra indicating H/D exchange of compound **4** on 500 MHz in CDCl_3 .

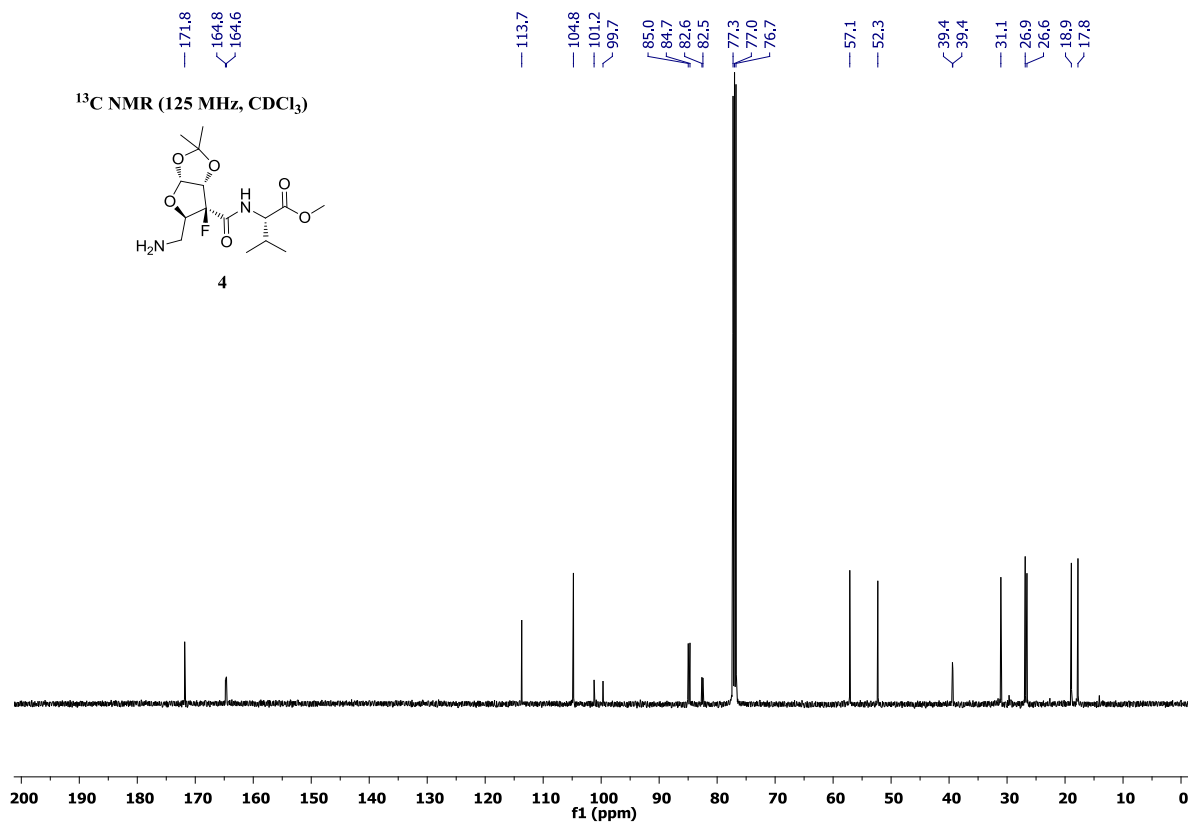


Figure S5: ¹³C NMR spectra of compound **4** on 125 MHz in CDCl₃.

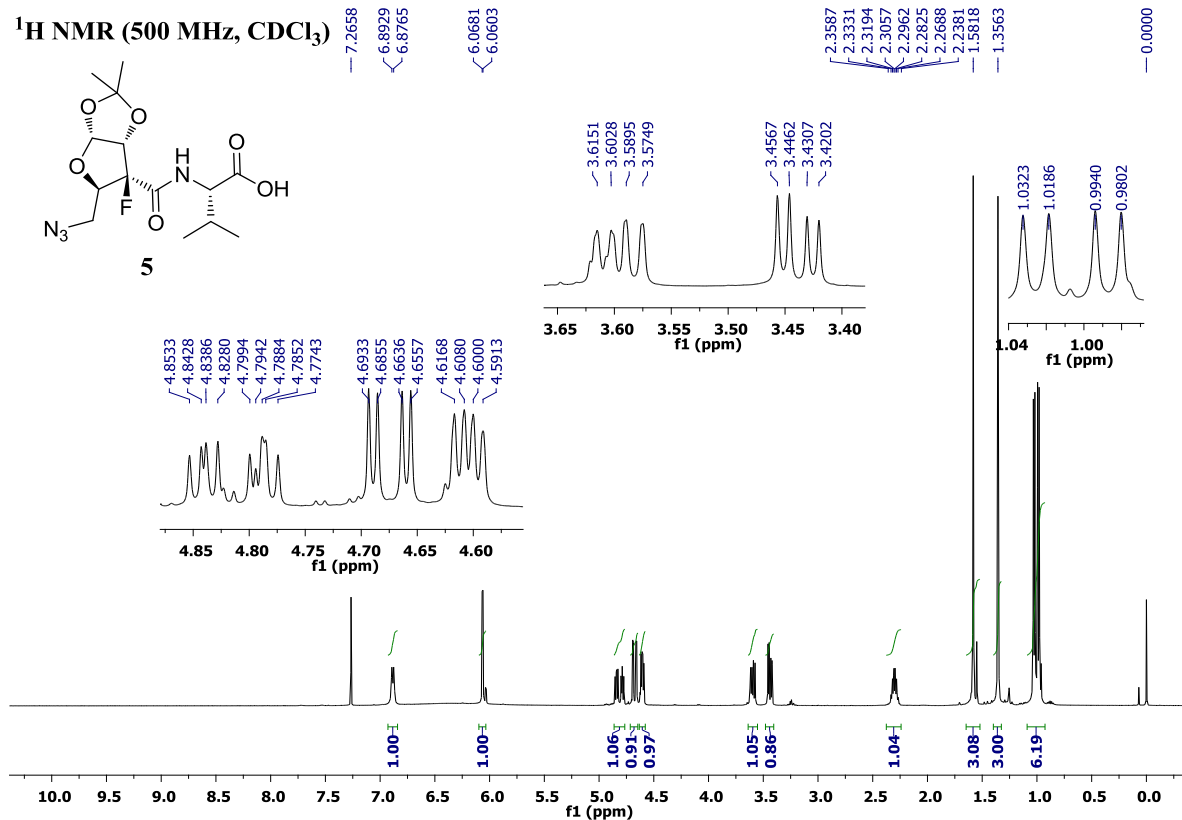


Figure S6: ¹H NMR spectra of compound **5** on 500 MHz in CDCl₃.

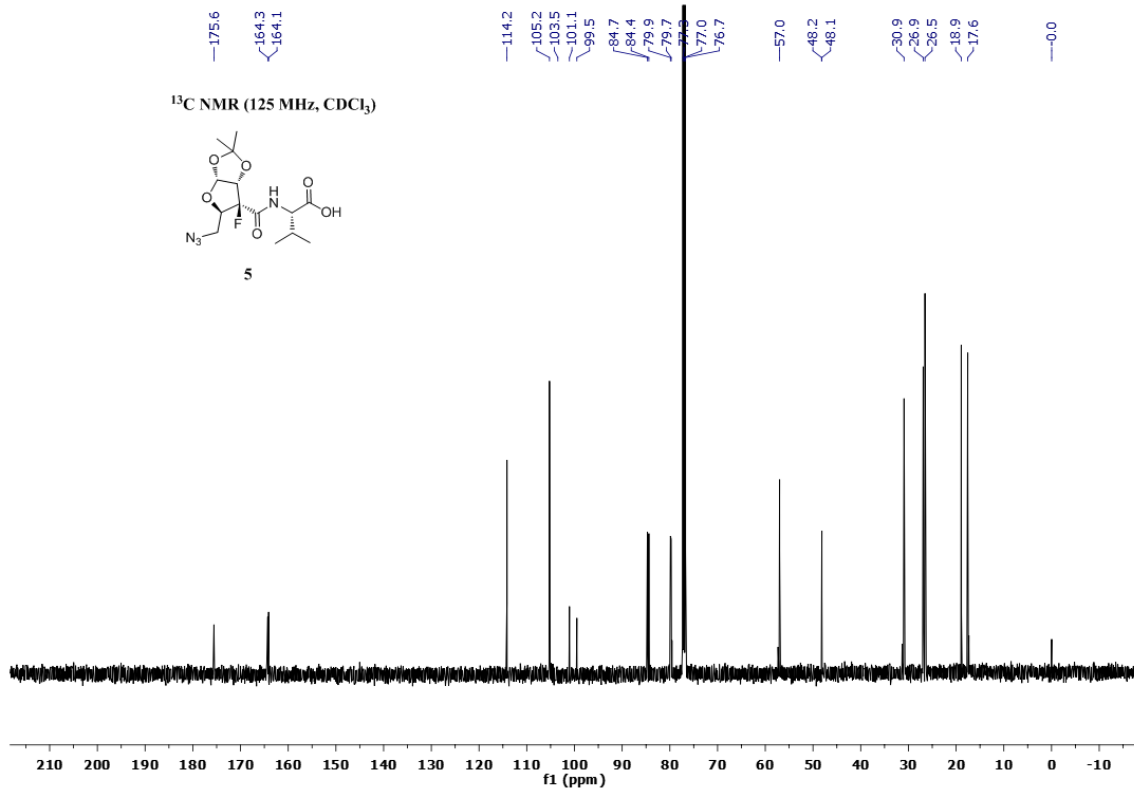


Figure S7: ¹³C NMR spectra of compound **5** on 125 MHz in CDCl₃.

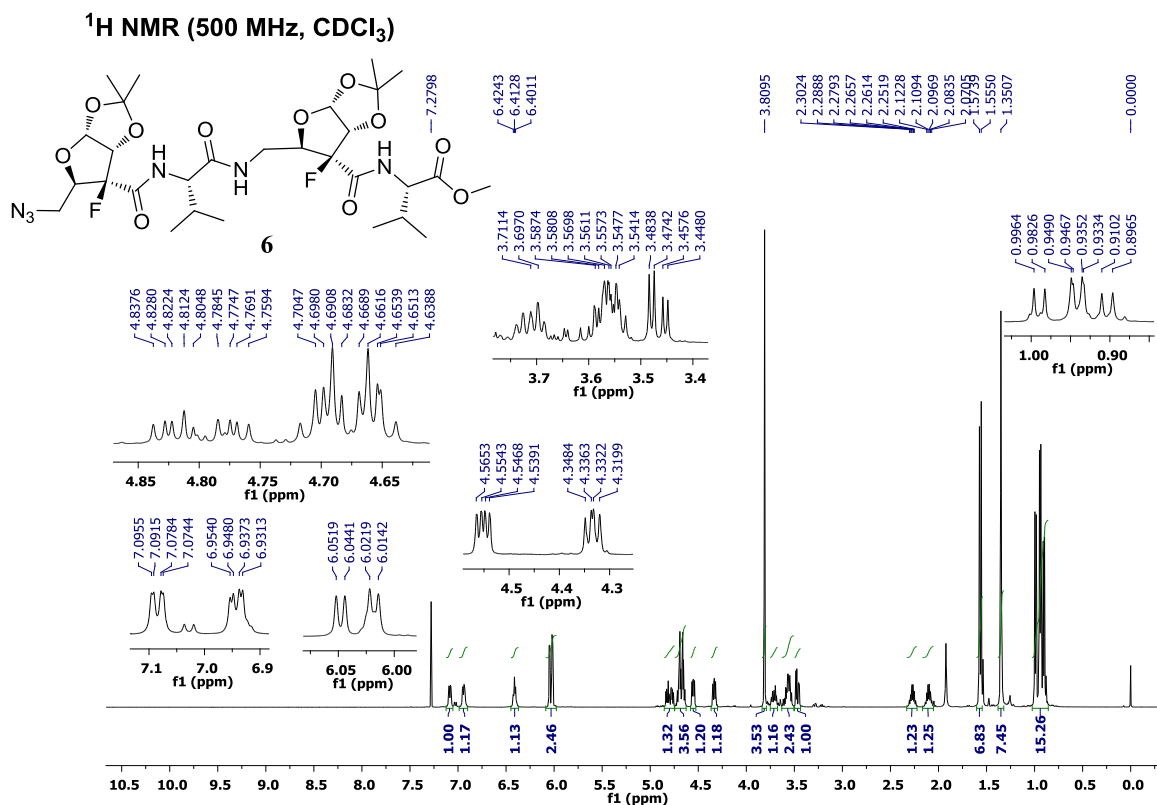


Figure S8: ¹H NMR spectra of compound **6** on 500 MHz in CDCl₃.

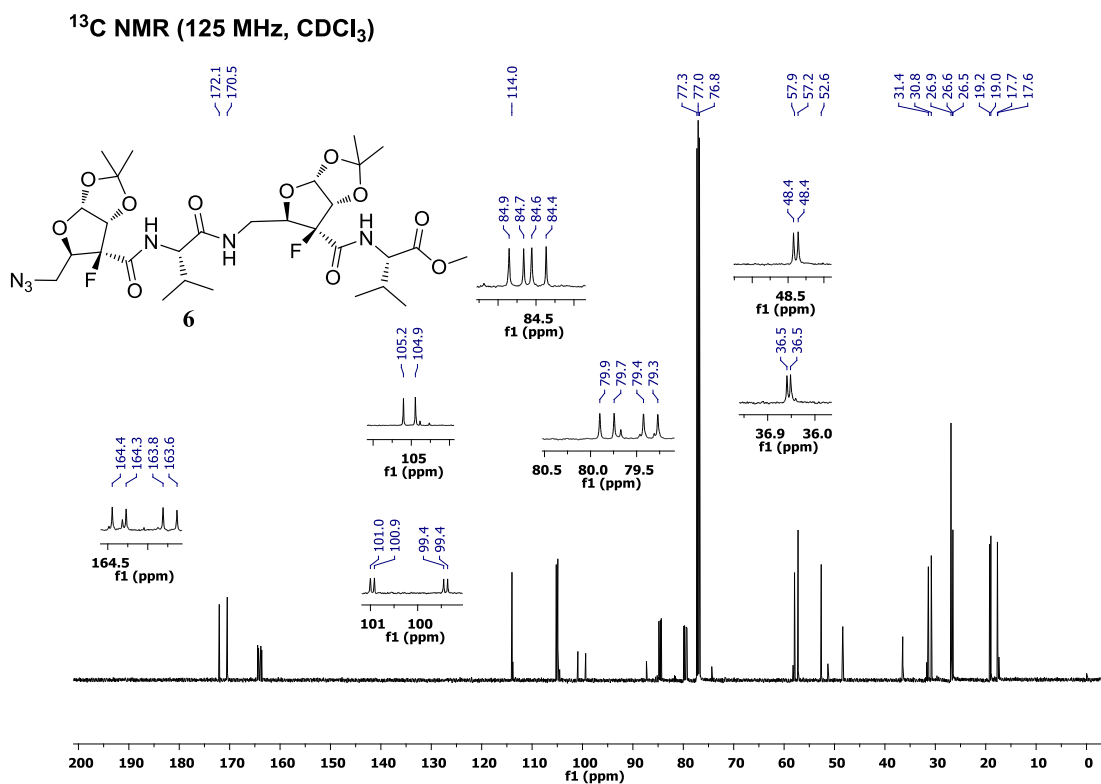


Figure S9: ¹³C NMR spectra of linear tetrapeptide **6** on 125 MHz in CDCl₃.

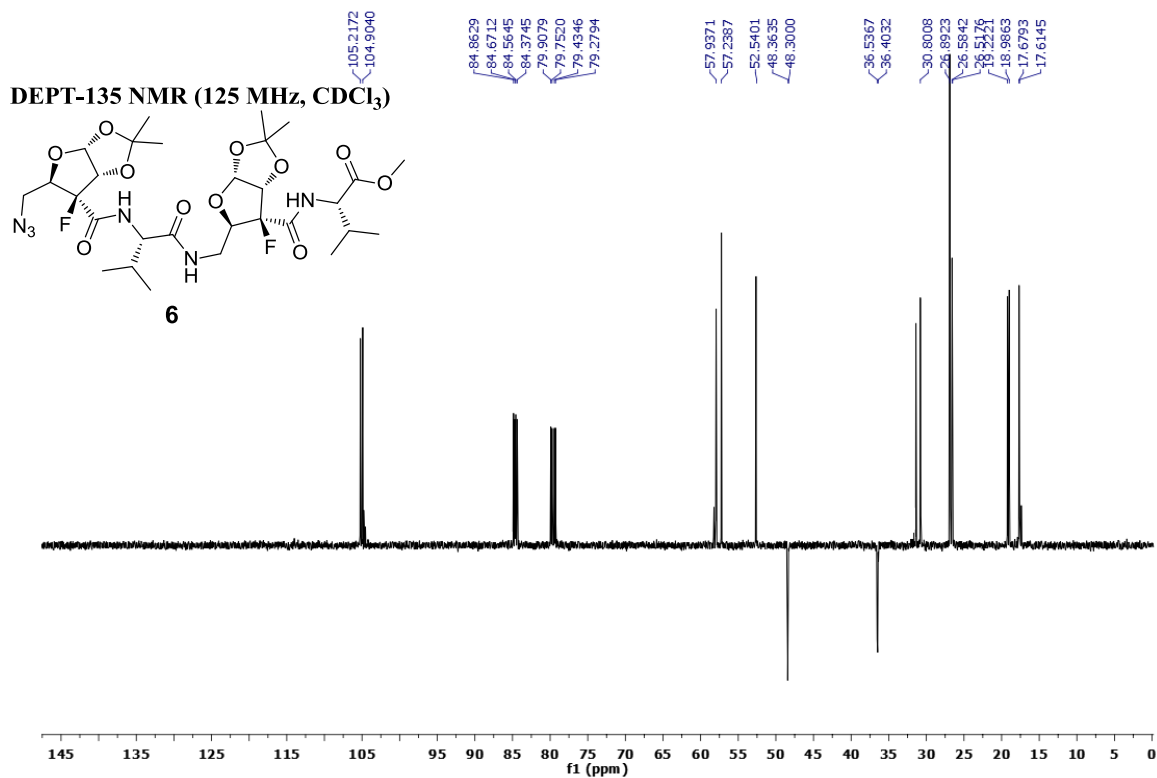


Figure S10: DEPT-135 NMR spectra of compound **6** on 125 MHz in CDCl₃.

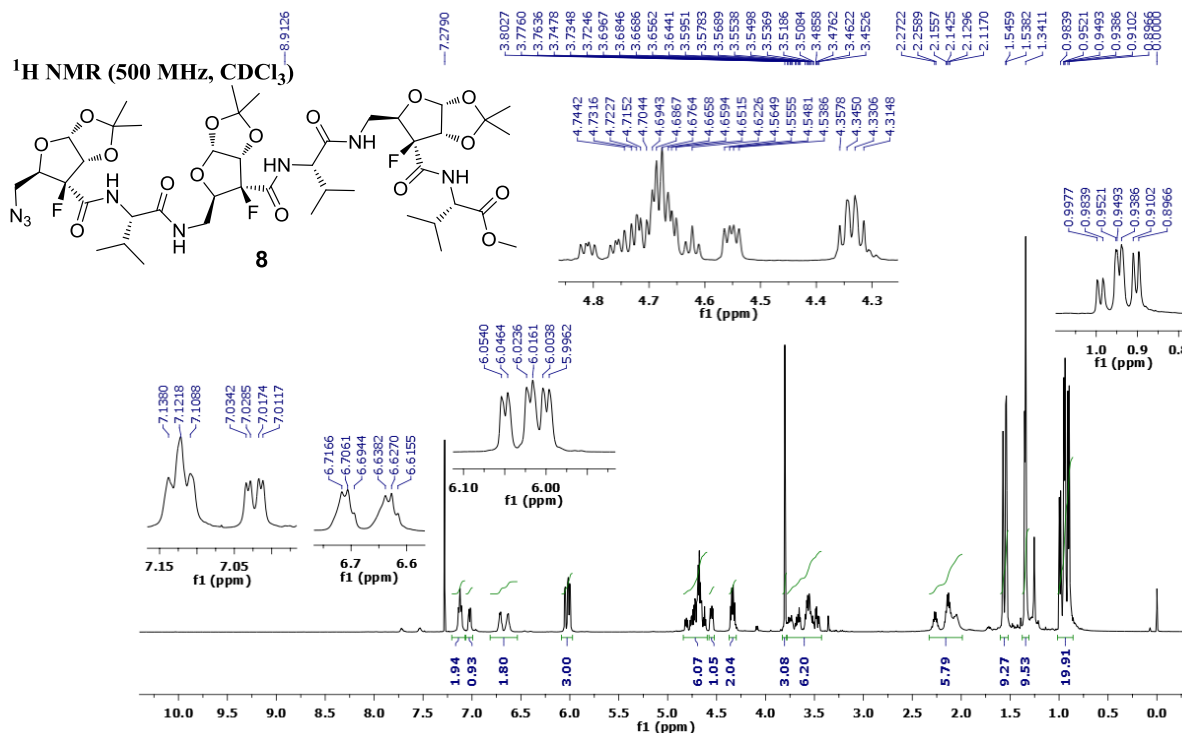


Figure S11: ¹H NMR spectra of linear hexapeptide **8** on 500 MHz in CDCl₃.

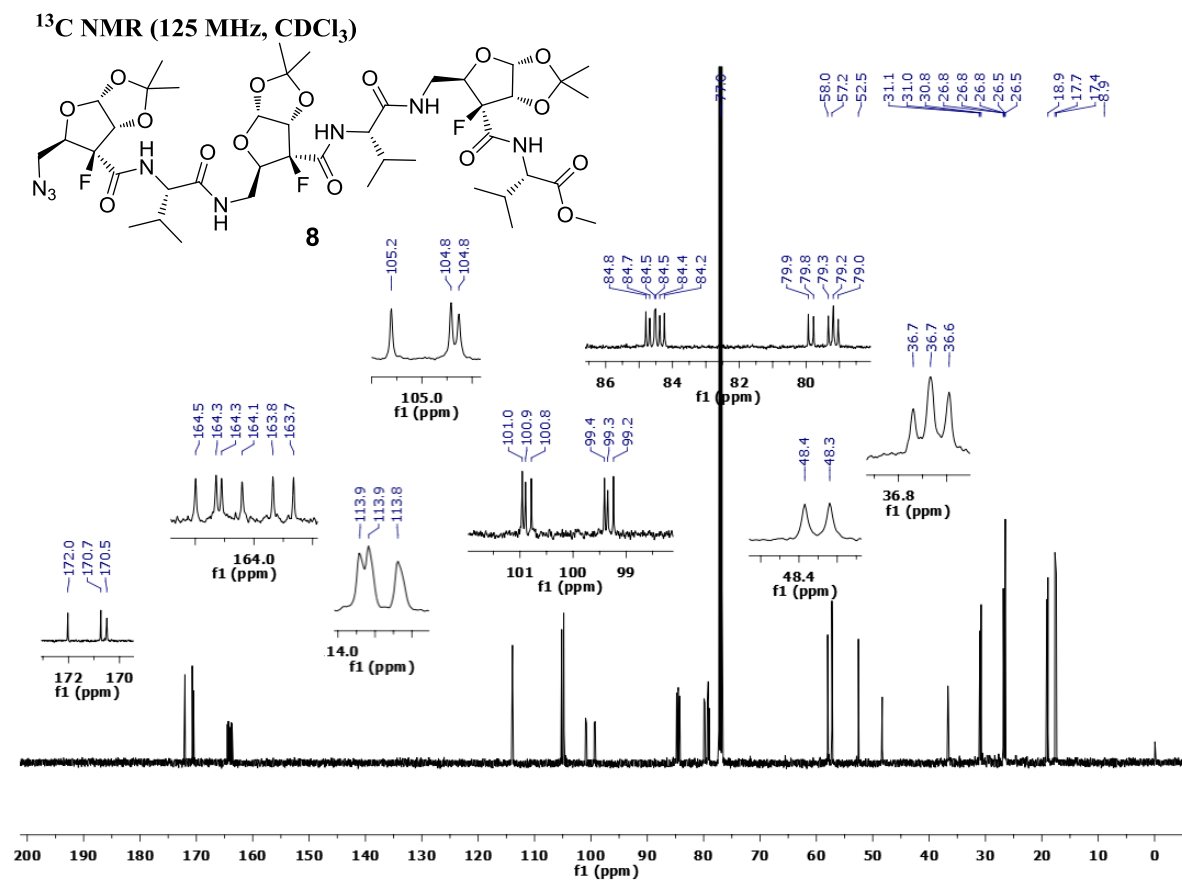


Figure S12: ¹³C NMR spectra of linear hexapeptide **8** on 125 MHz in CDCl₃.

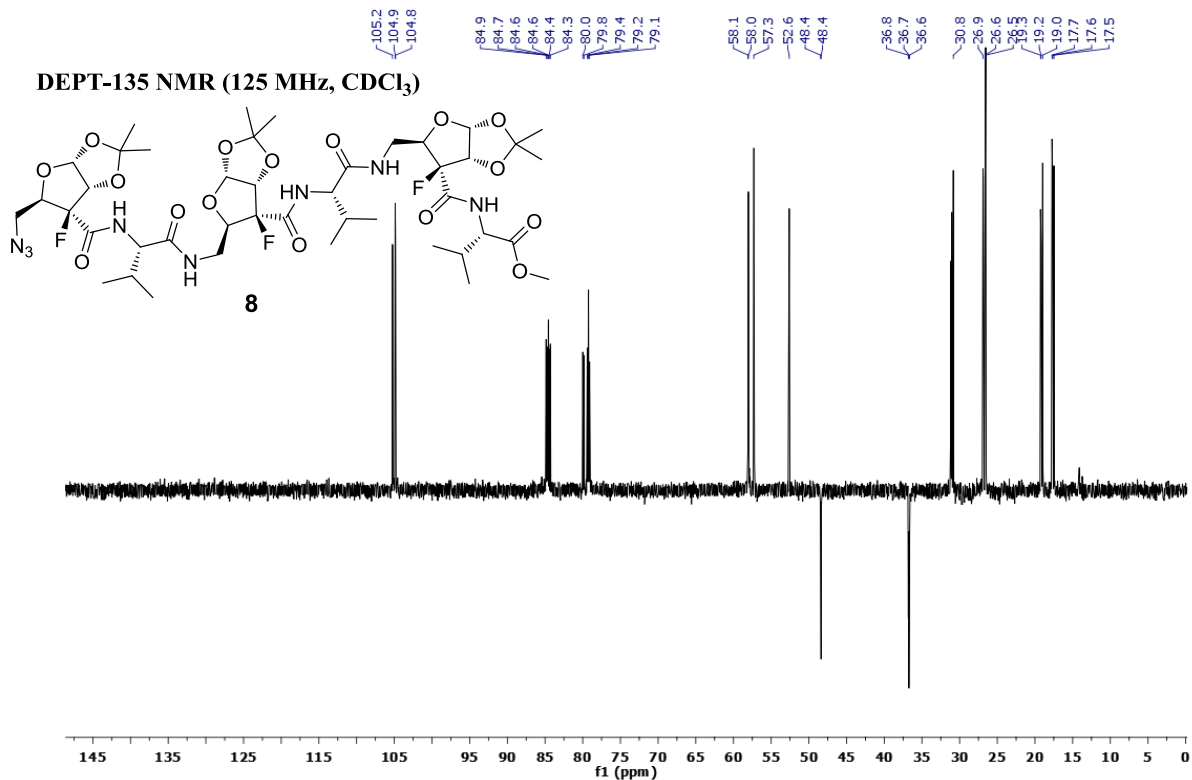


Figure S13: DEPT-135 NMR spectra of compound **8** on 125 MHz in CDCl₃.

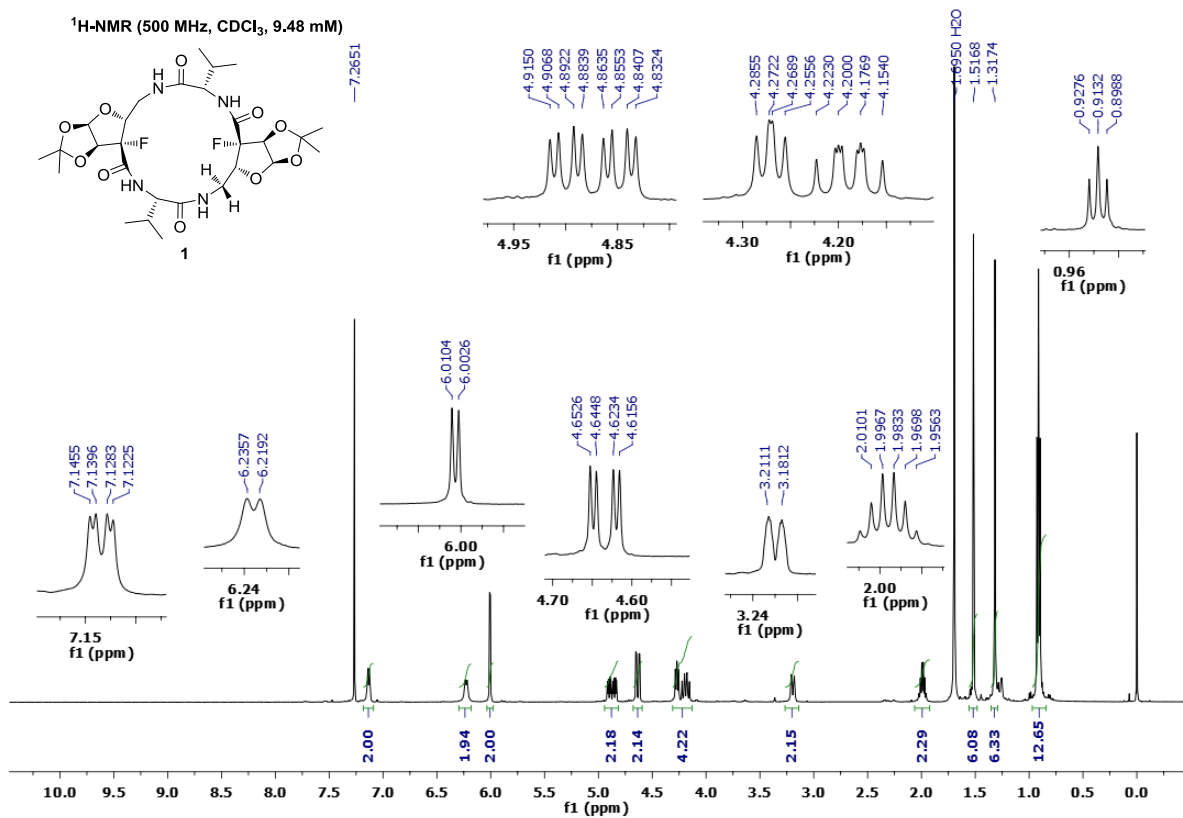


Figure S14: ¹H NMR spectra of fluorinated α , γ -cyclic tetrapeptide **1** on 500 MHz in CDCl₃.

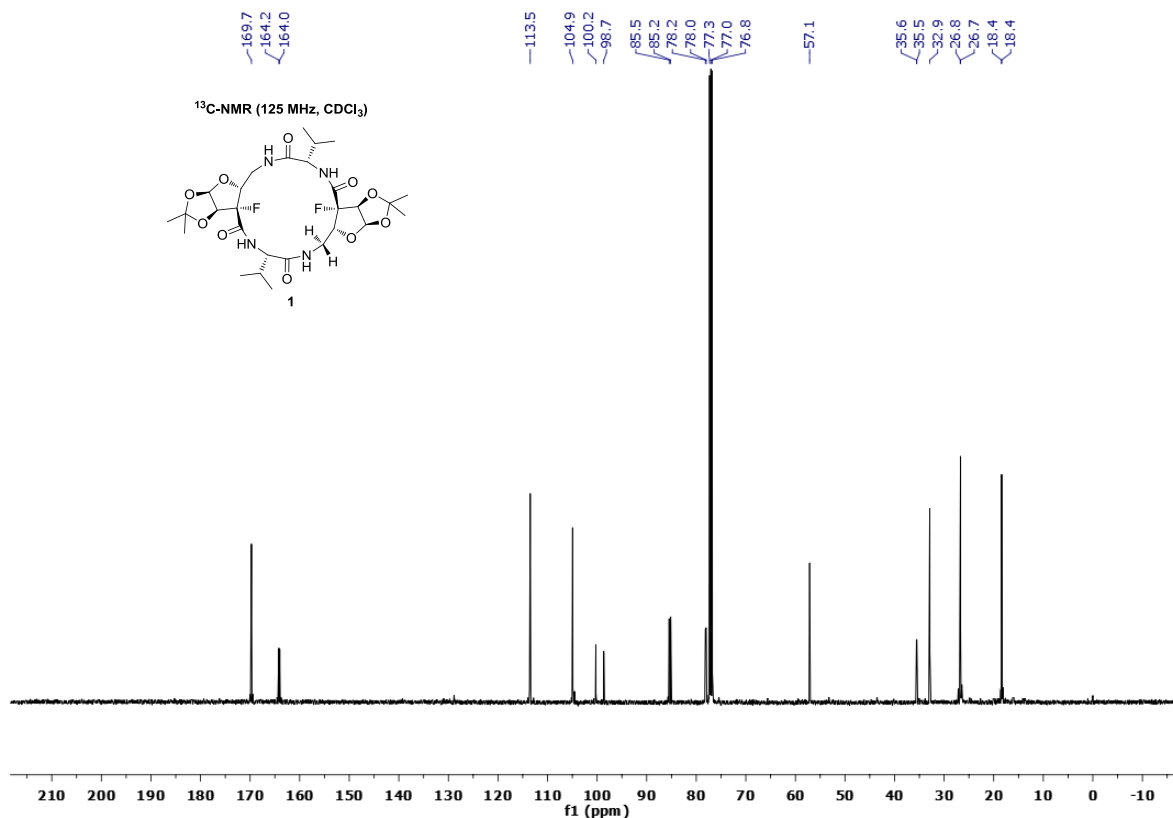


Figure S15: ¹³C NMR spectra of fluorinated α , γ -cyclic tetrapeptide **1** on 125 MHz in CDCl₃.

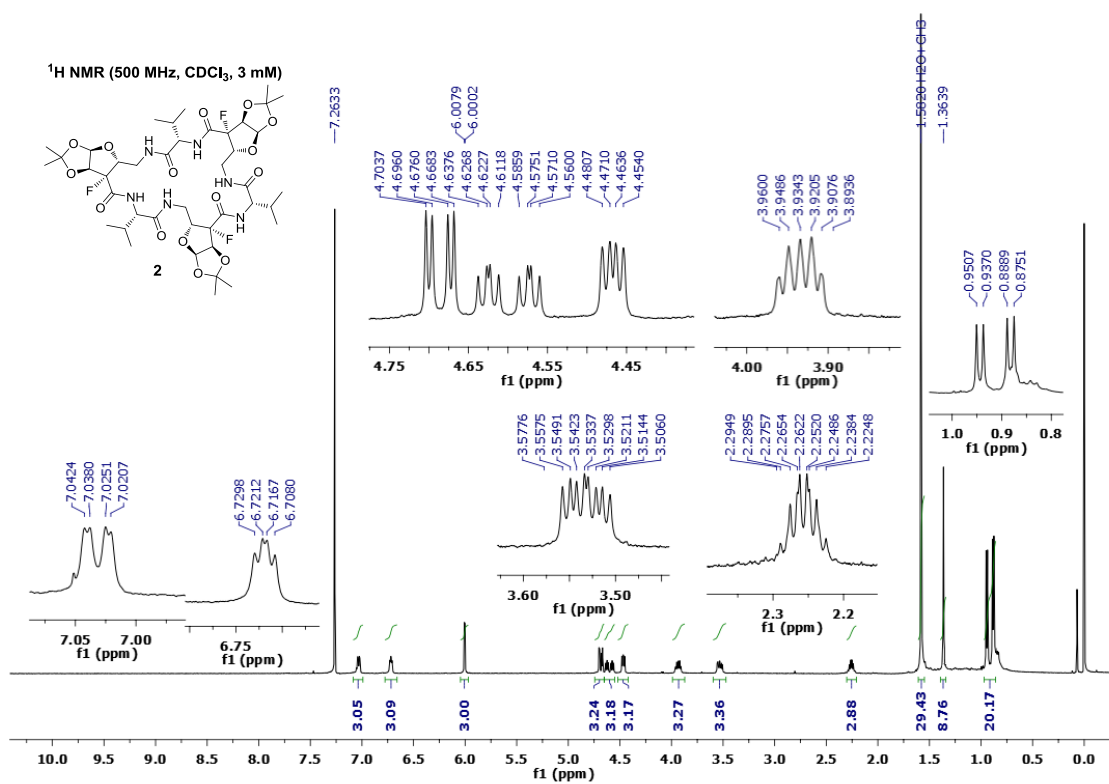


Figure S16: ¹H NMR spectra of fluorinated α , γ -cyclic hexapeptide **2** on 500 MHz in CDCl₃.

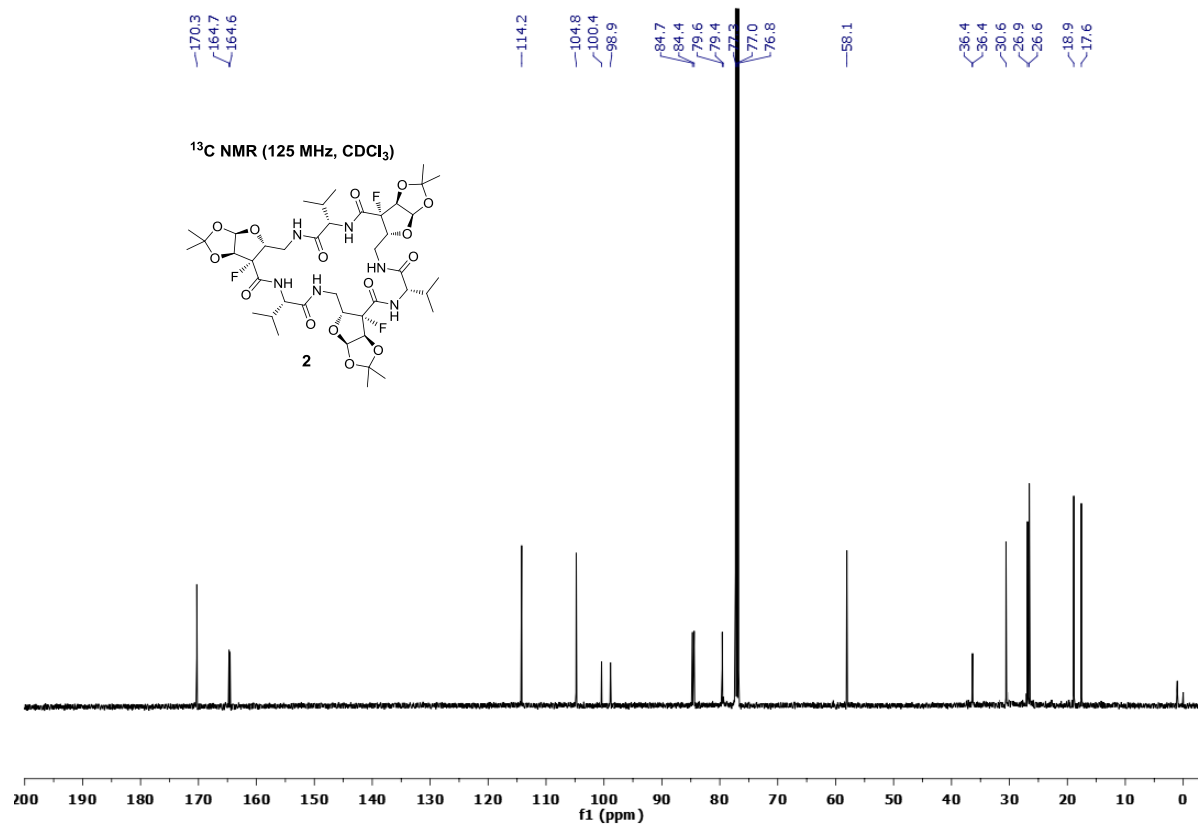


Figure S17: ¹³C NMR spectra of fluorinated α, γ -cyclic hexapeptide **2** on 125 MHz in CDCl₃.

7. 2D NMR Spectra:

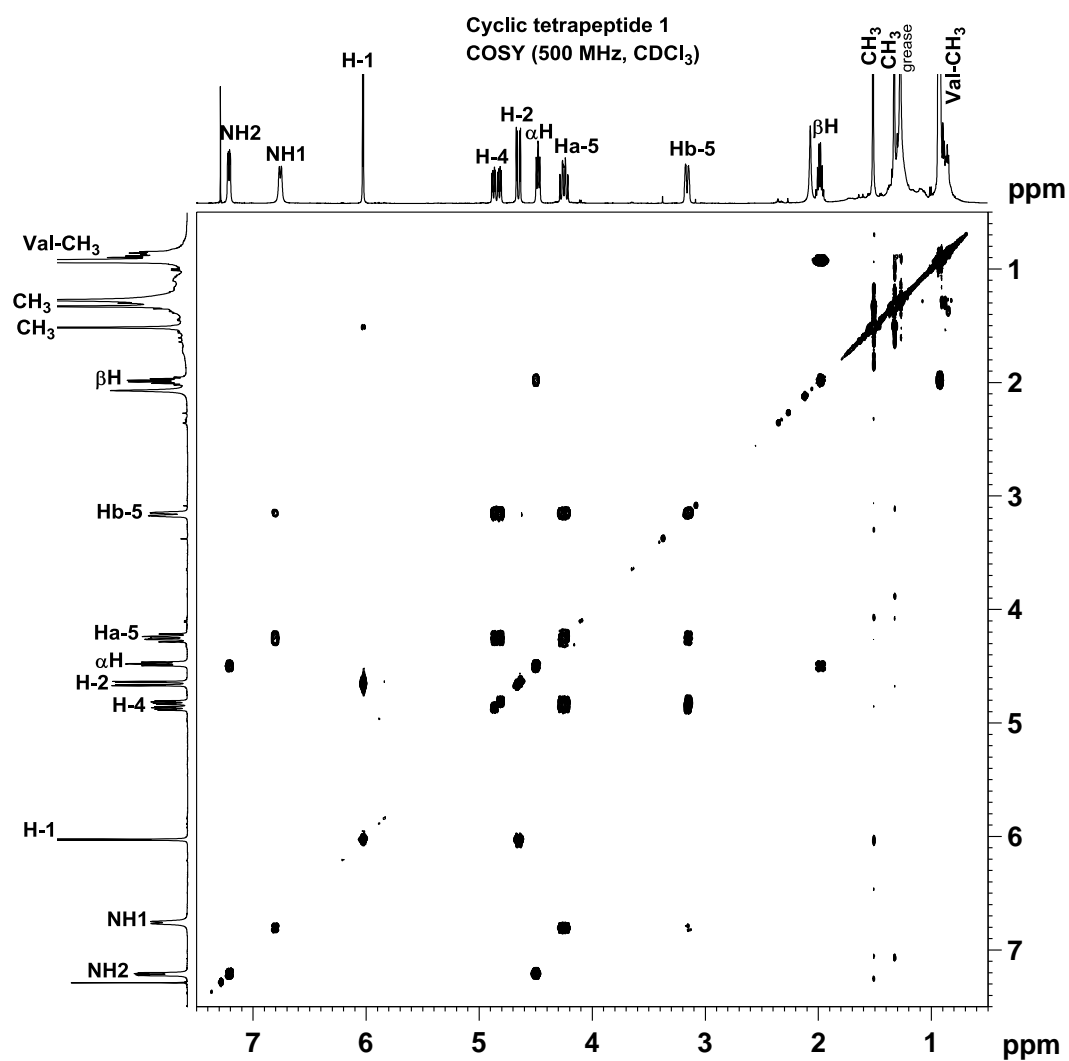


Figure S18: ^1H - ^1H COSY NMR spectra of fluorinated α,γ -cyclic tetrapeptide **1** on 500 MHz in CDCl₃.

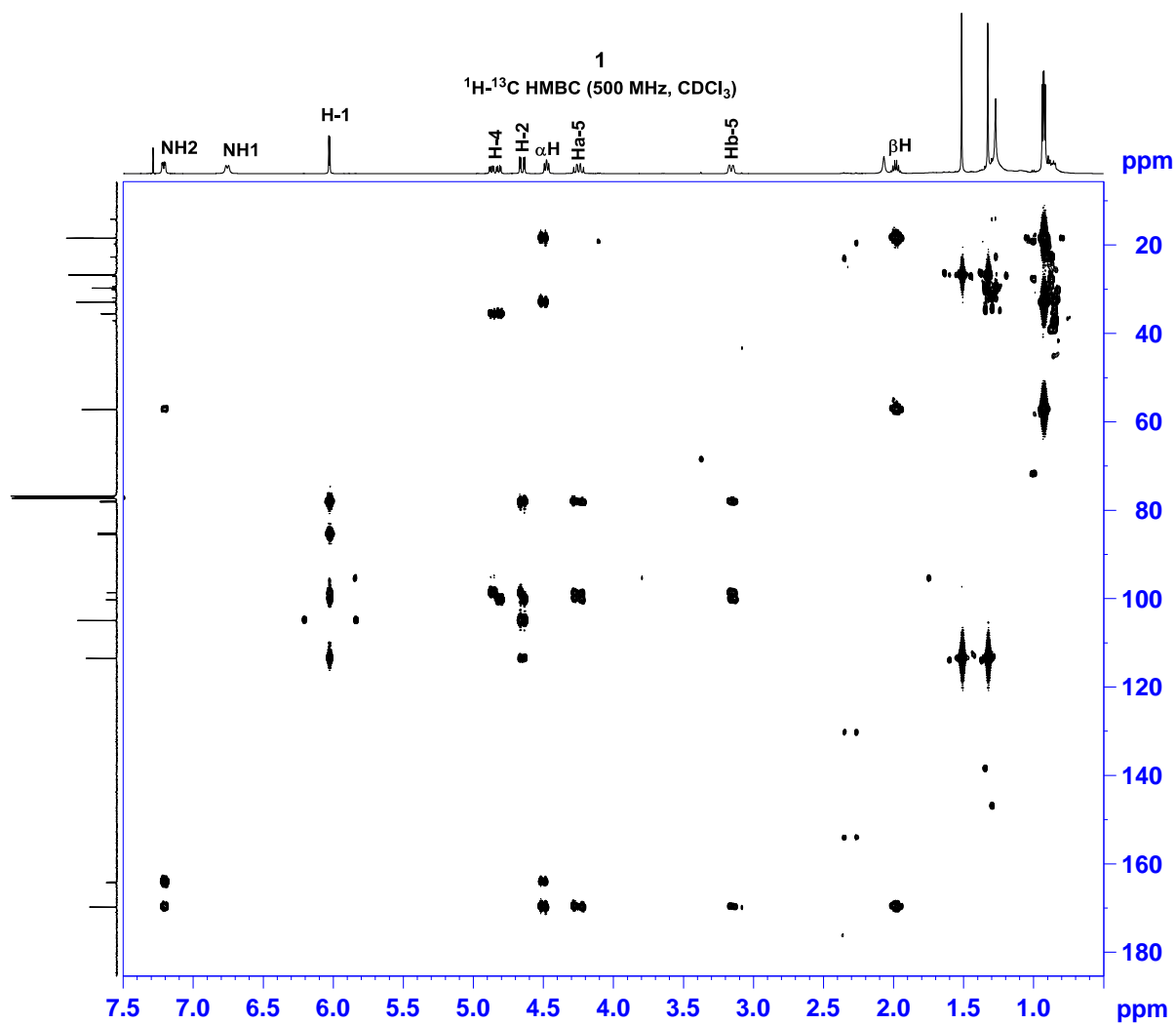


Figure S19: HMBC NMR spectra of fluorinated α,γ -cyclic tetrapeptide **1** on 500 MHz in CDCl₃.

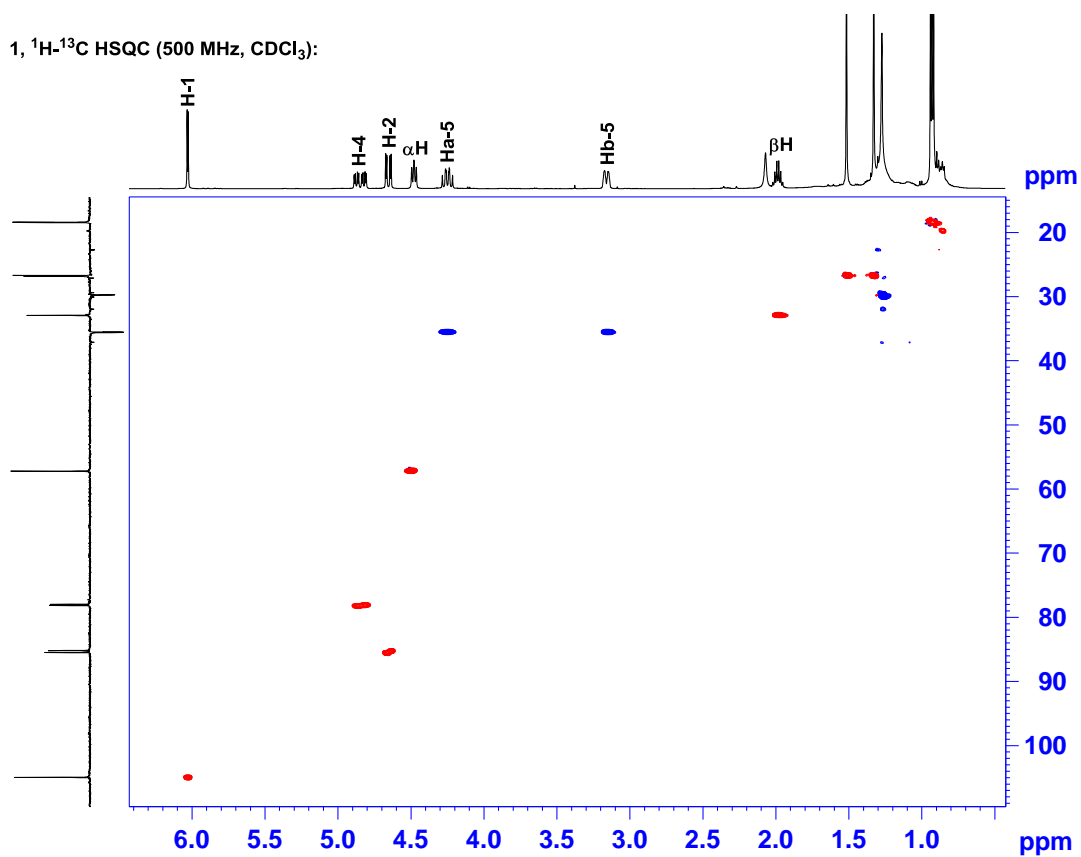


Figure S20: HSQC NMR spectra of fluorinated α,γ -cyclic tetrapeptide **1** on 500 MHz in CDCl_3 .

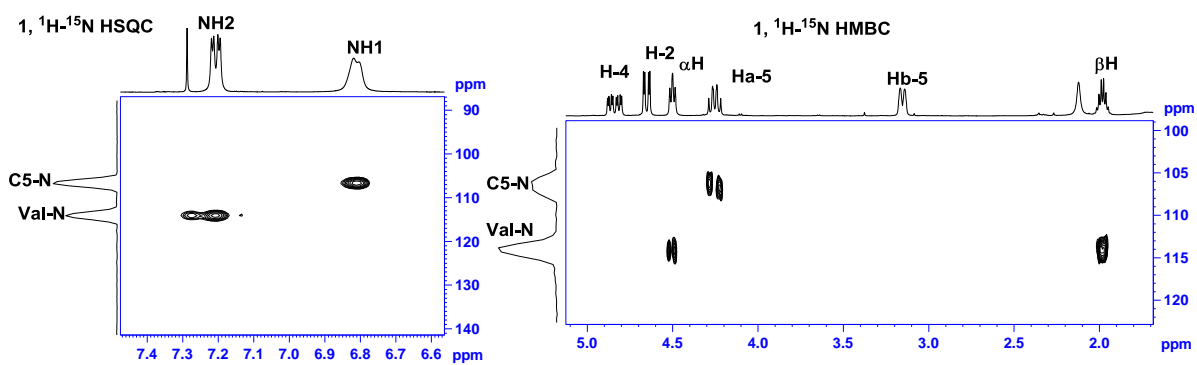


Figure S21: ^1H - ^{15}N HMBC and HSQC NMR spectra of fluorinated α,γ -cyclic tetrapeptide **1** on 500 MHz in CDCl_3 .

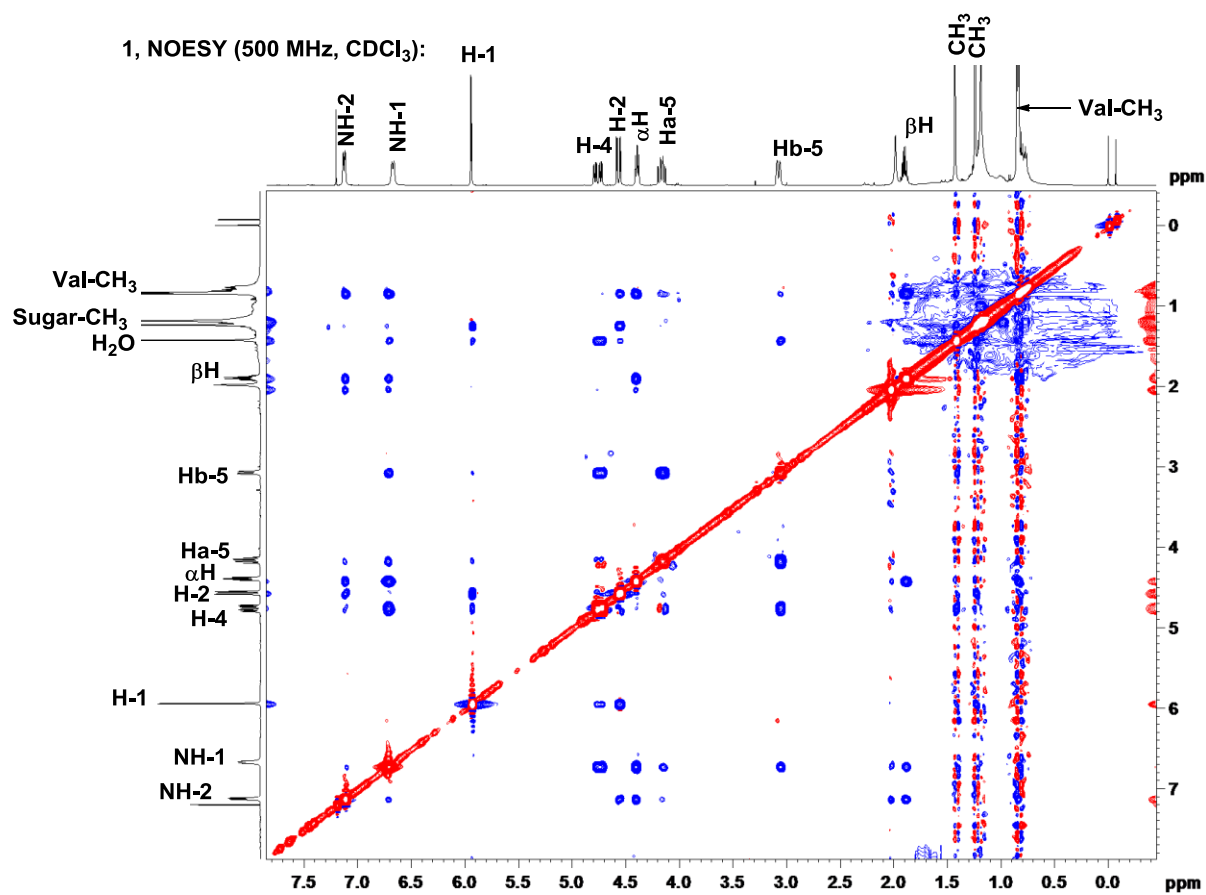


Figure S22: ^1H - ^1H NOESY NMR spectra of fluorinated α,γ -cyclic tetrapeptide **1** on 500 MHz in CDCl₃.

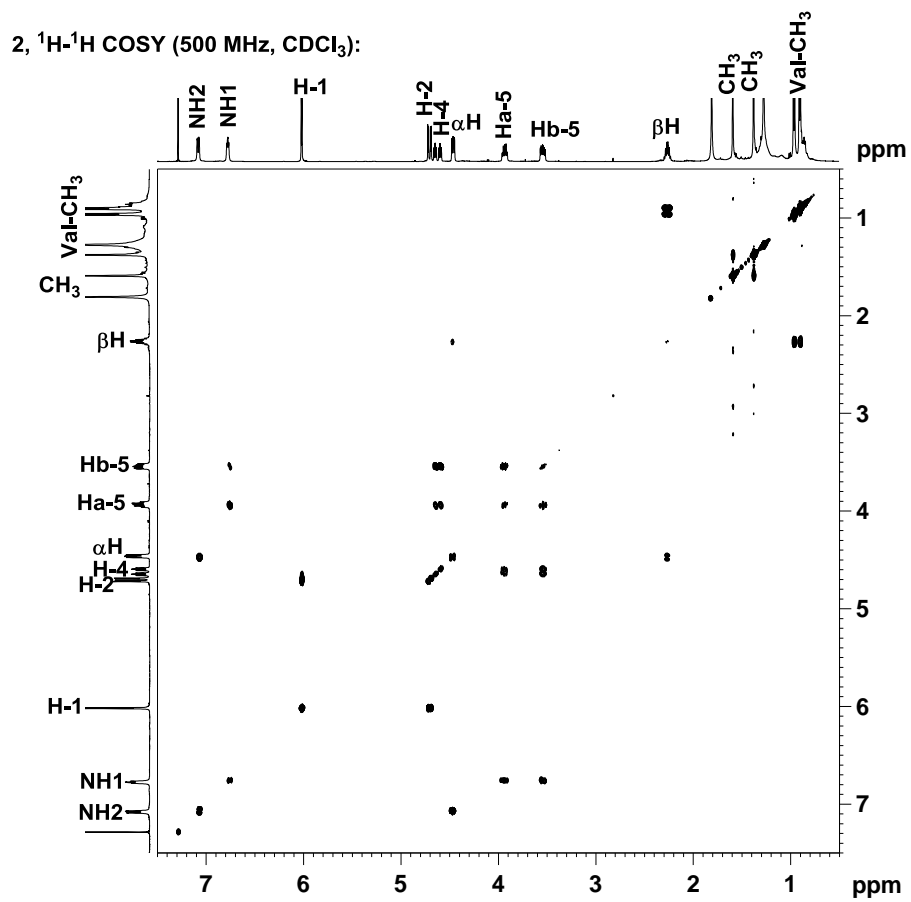


Figure S23: ^1H - ^1H COSY NMR spectra of fluorinated α,γ -cyclic hexapeptide **2** on 500 MHz in CDCl_3 .

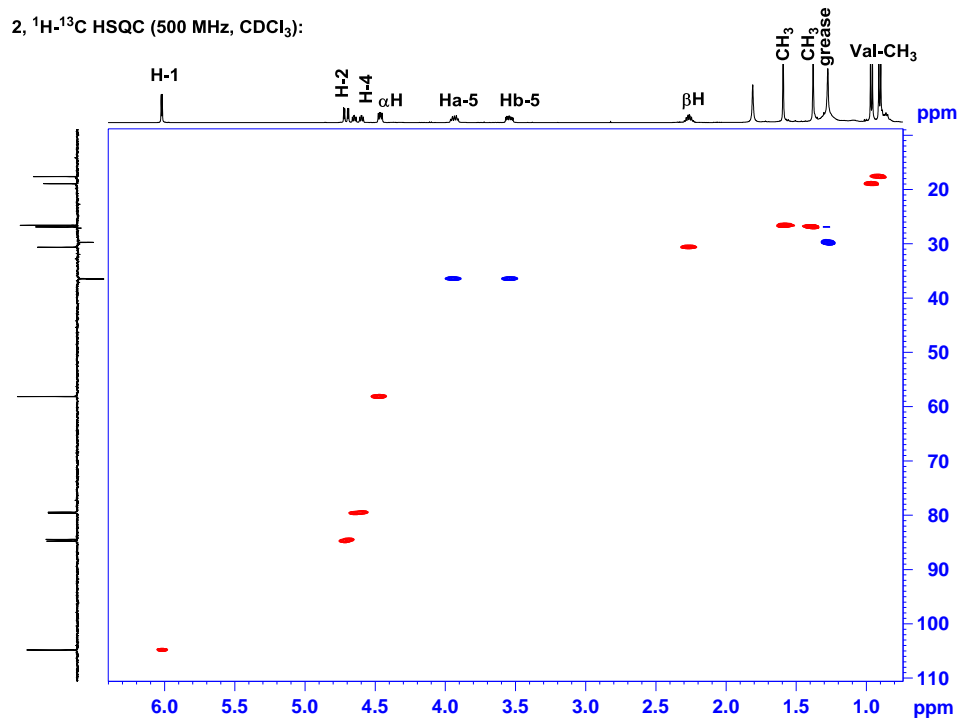


Figure S24: HSQC NMR spectra of fluorinated α,γ -cyclic hexapeptide **2** on 500 MHz in CDCl_3 .

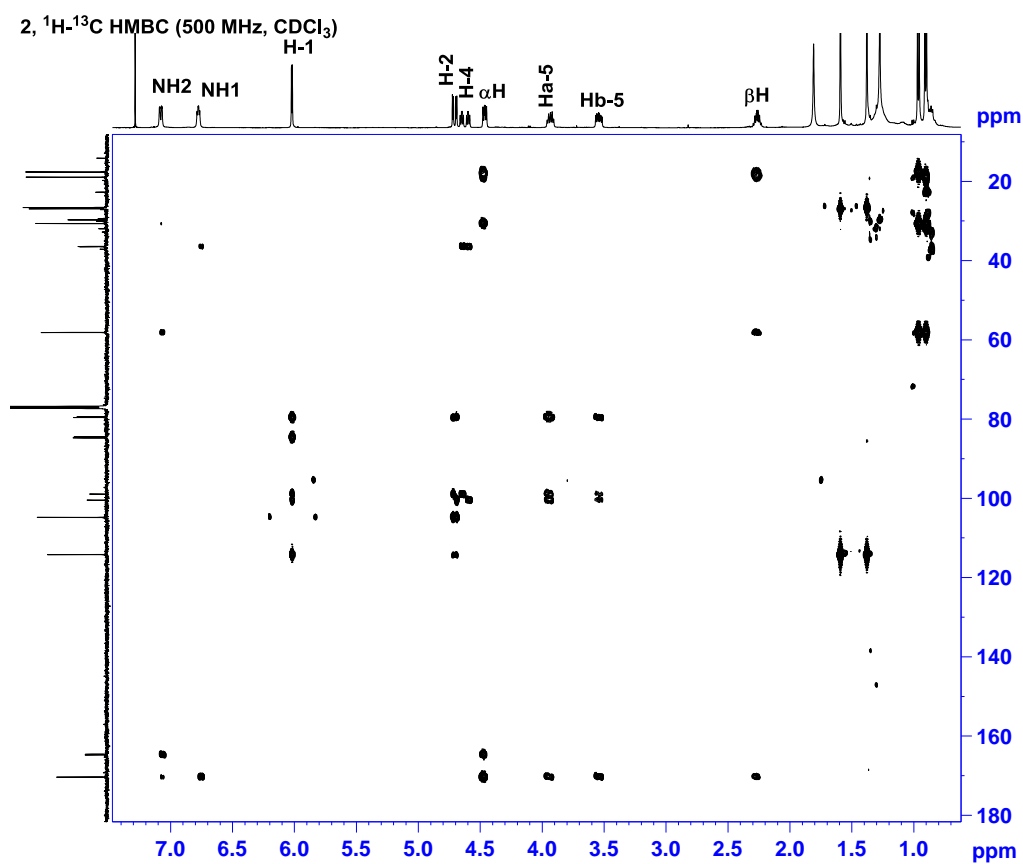


Figure S25: HMBC spectra of fluorinated α,γ -cyclic hexapeptide **2** on 500 MHz in CDCl_3 .

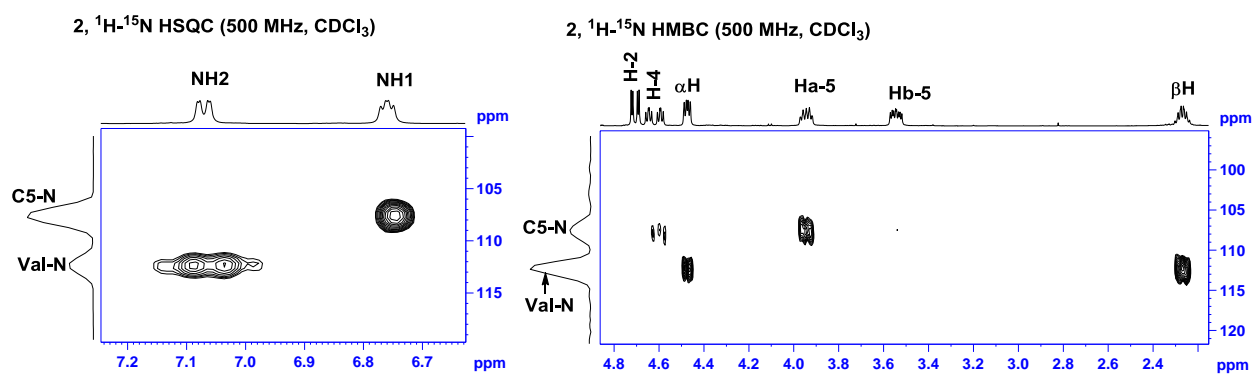


Figure S26: ^1H - ^{15}N HSQC and HMBC NMR spectra of fluorinated α,γ -cyclic hexapeptide **2** on 500 MHz in CDCl_3 .

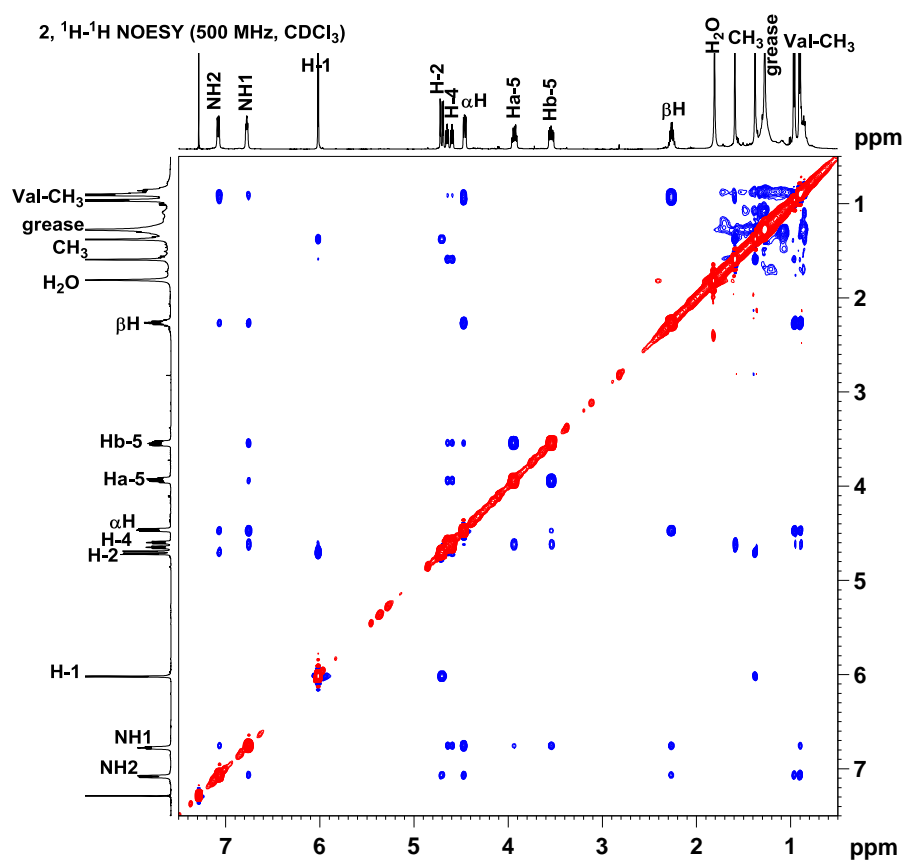


Figure S27: ^1H - ^1H NOESY NMR spectra of fluorinated α,γ -cyclic hexapeptide **2** on 500 MHz in CDCl_3 .

8. Schematic NOESY representation:

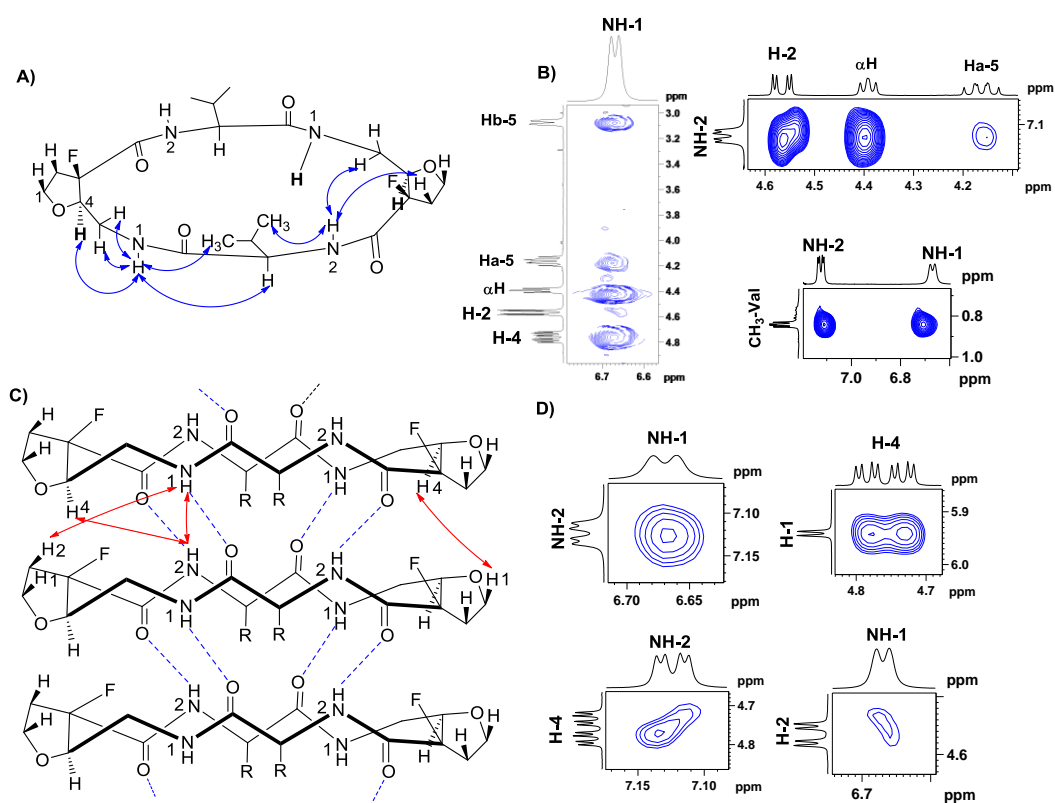


Figure S28: Characteristic NOEs representation of FCTP 1: observed strong NOEs due to the possible intra-molecular interactions (shown in blue arrow) in monomeric structure (A and B) and weak NOEs between *trans* proton due to the possible inter-molecular interaction (shown in red arrow) in self-assembled β -sheet structure (C and D).

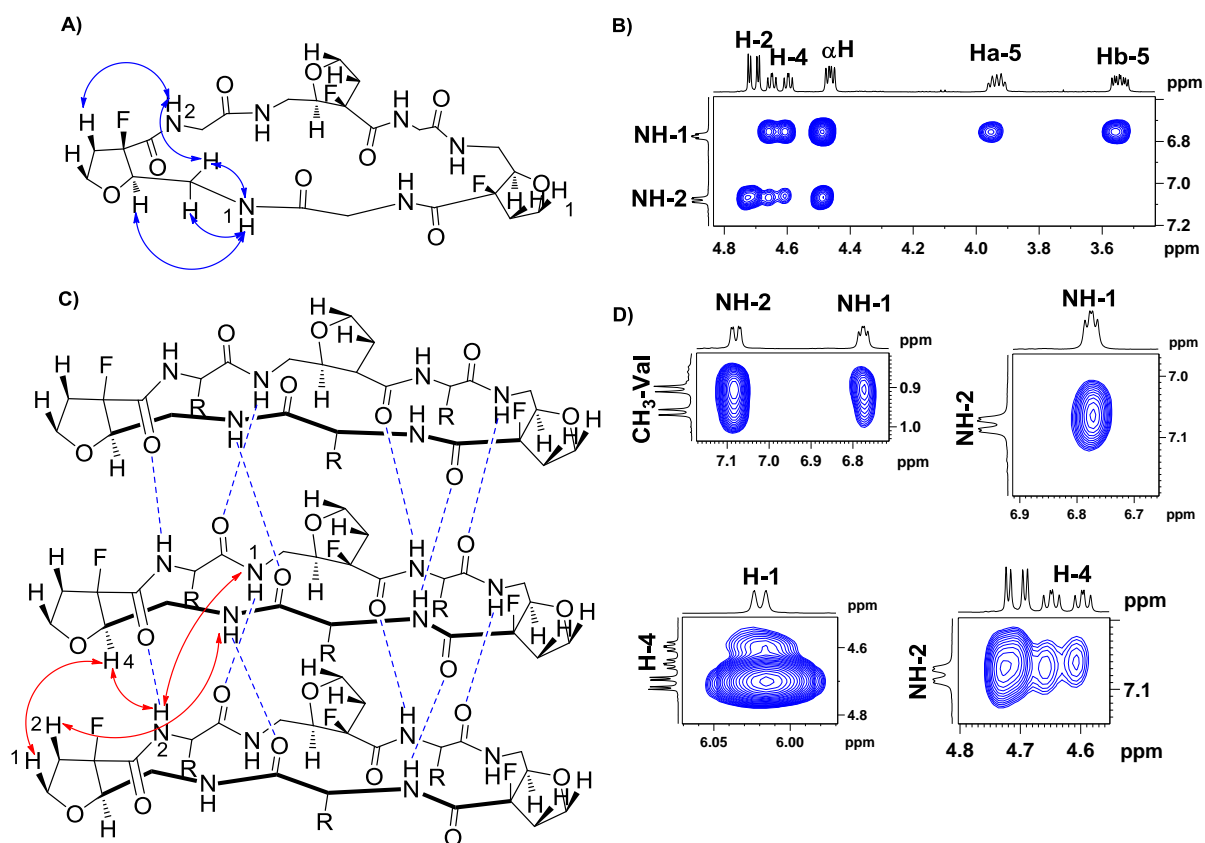


Figure S29: Characteristic NOEs representation of FCHP 2: observed strong NOEs due to the possible intra-molecular interaction (shown in blue arrow) in monomeric structure (A and B) and weak NOEs between *trans* proton due to the possible inter-molecular interaction (shown in red arrow) in self-assembled β -sheet structure (C and D).

9. HOESY NMR spectra:

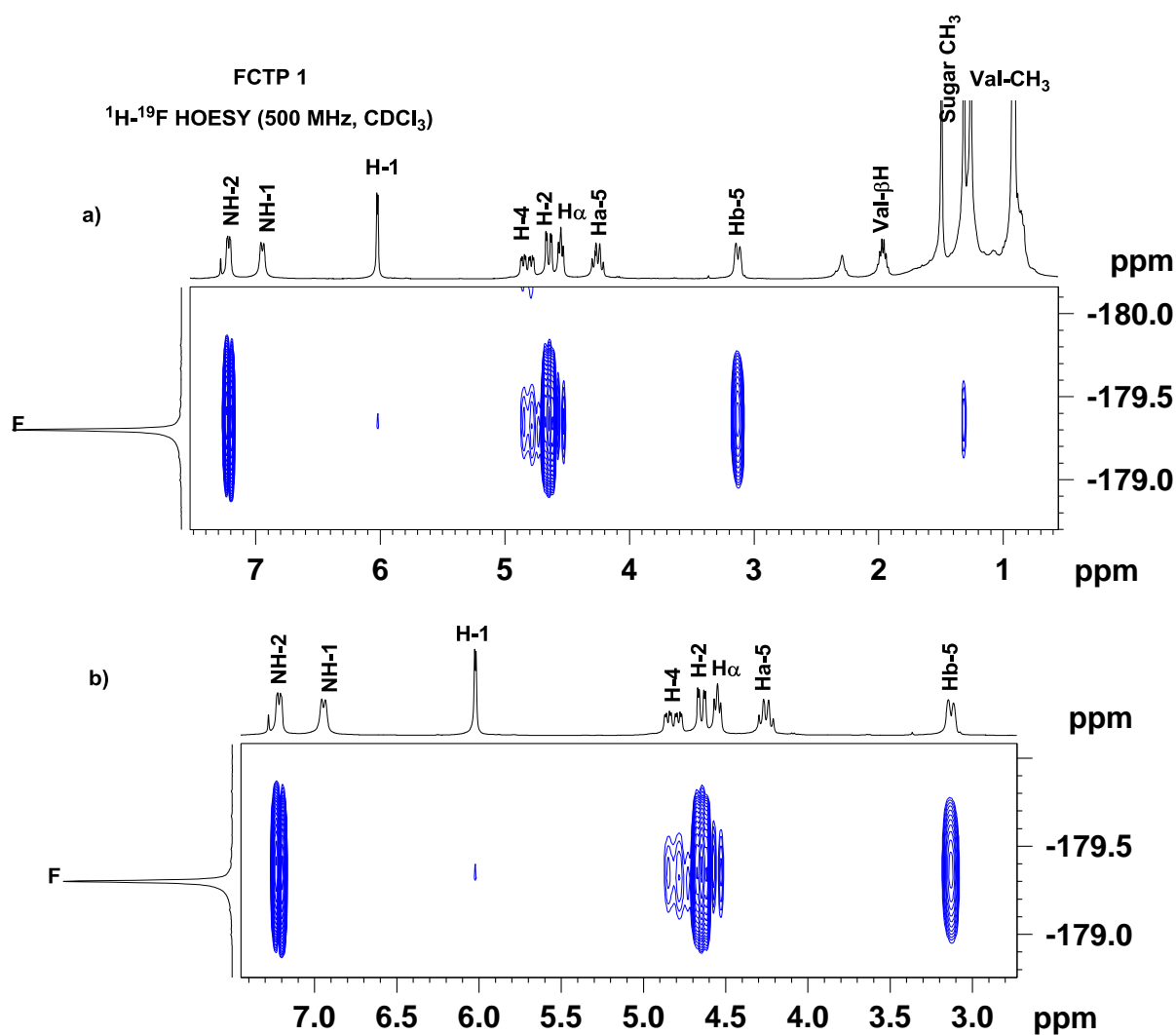


Figure S30: ^1H - ^{19}F HOESY NMR spectra in CDCl_3 (500 MHz) of fluorinated α,γ -cyclic tetrapeptide **1**.

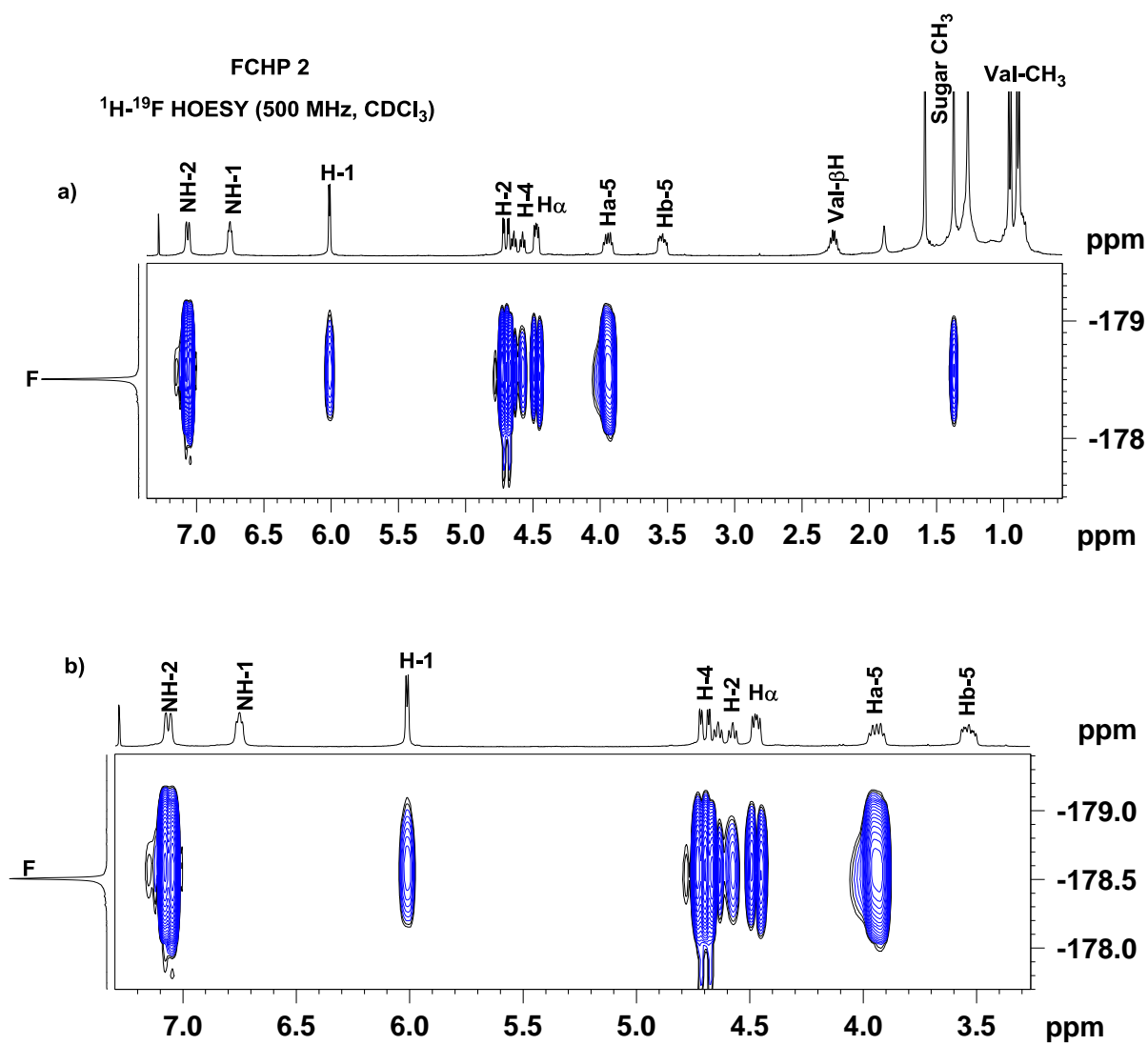


Figure S31: ^1H - ^{19}F HOESY NMR spectra in CDCl_3 (500 MHz) of fluorinated α,γ -cyclic hexapeptide **2**.

10. Aggregation studies of **1** and **2** using concentration dependent NMR:

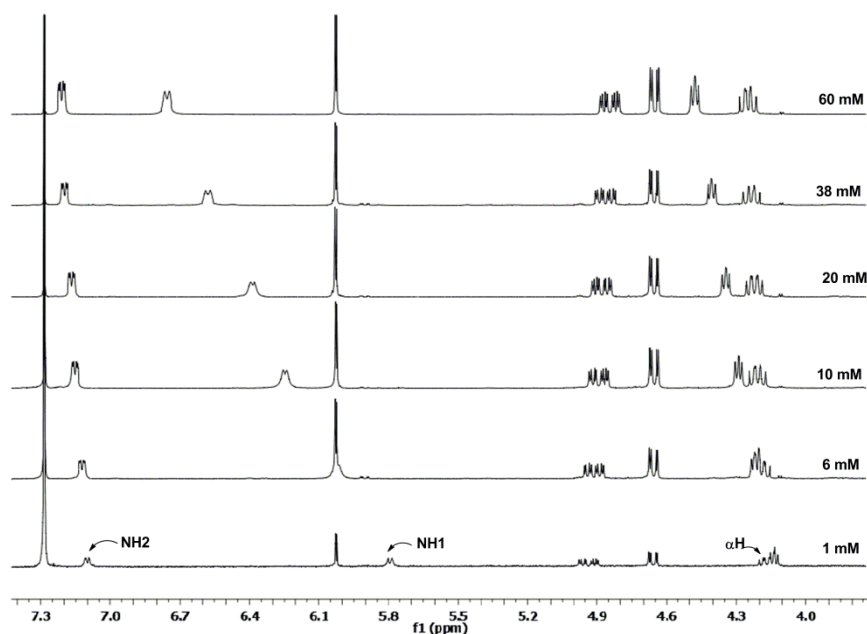


Figure S32: Selected region of $^1\text{H-NMR}$ spectra of **1** in CDCl_3 (500 MHz, probe temperature = 298 K) showed down field shift with increase in concentration (1 - 60 mM) for amide protons that supports the involvement of molecular aggregations in β -sheet structure.

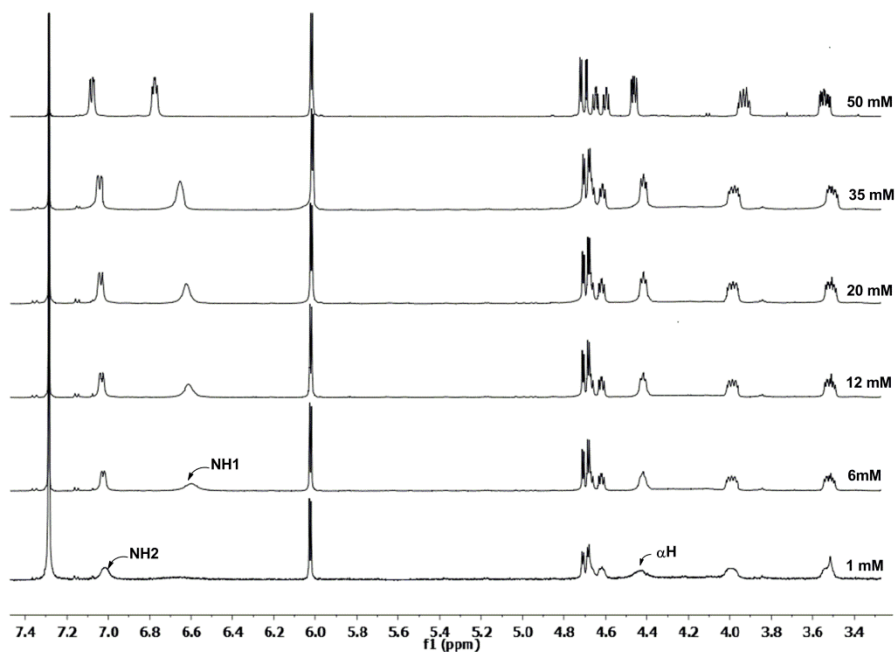


Figure S33: Selected region of $^1\text{H-NMR}$ spectra of **2** in CDCl_3 (500 MHz, probe temperature = 298 K) showed down field shift with increase in concentration (1 - 60 mM) for amide protons, which supports the involvement of molecular aggregations in β -sheet structure.

11. Aggregation studies of 1 and 2 by using ESI-MS:

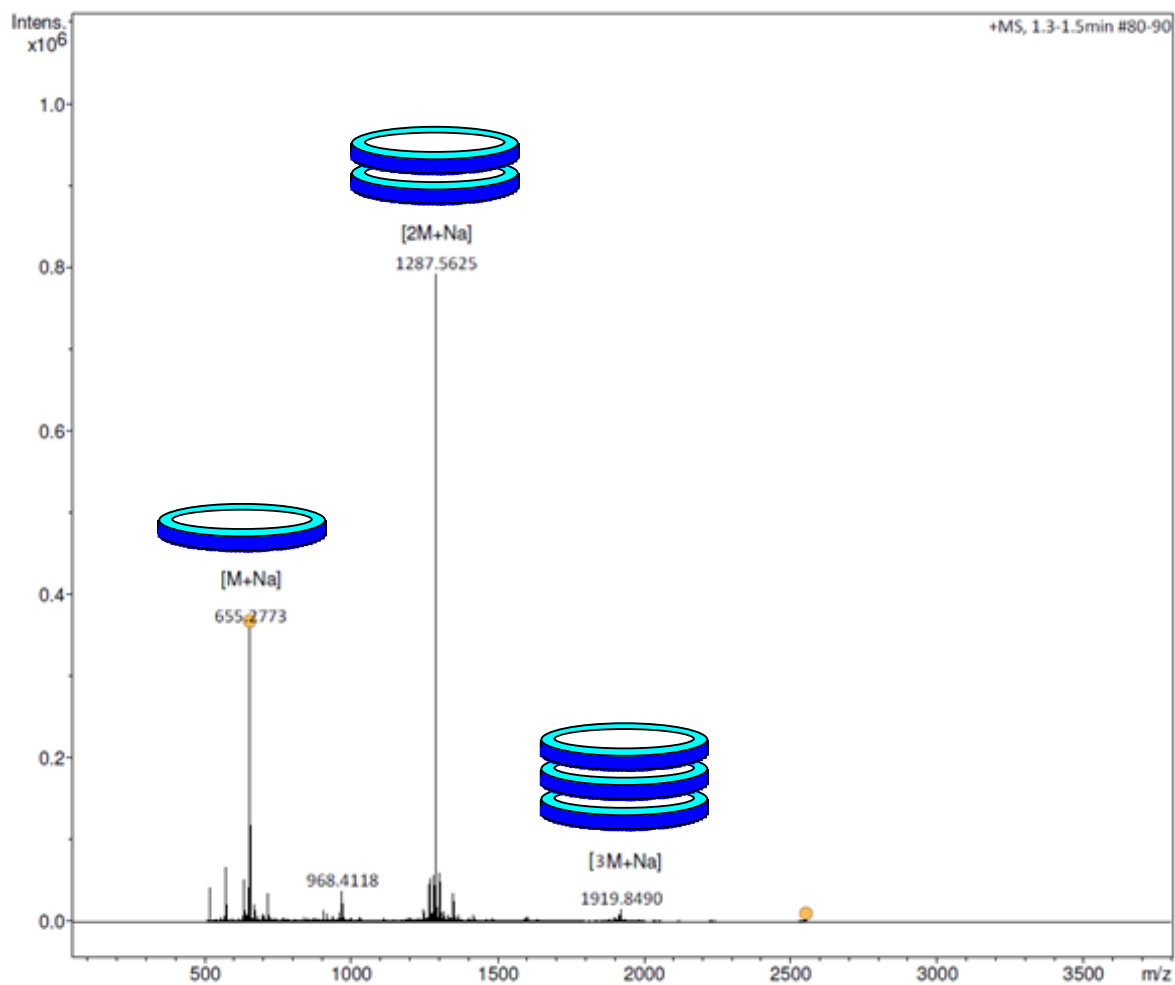


Figure S34: ESI-MS spectra of FCTP **1** indicated self-aggregated mass peaks due to monomer, dimer and trimer formation as shown in full spectrum and its expanded region.

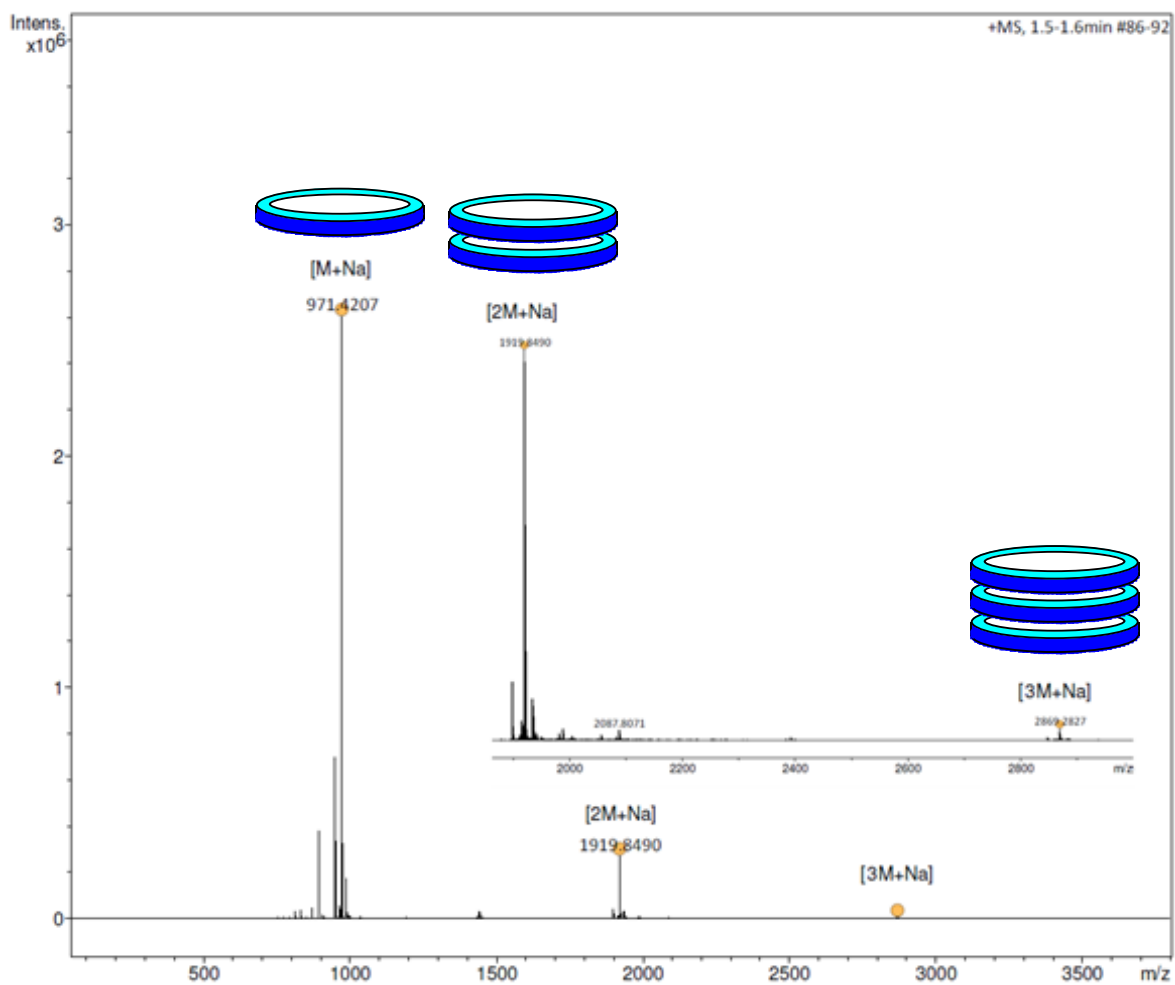


Figure S35: ESI-MS spectra of FCHP 2 indicated self-aggregated mass peaks due to monomer, dimer and trimer formation as shown in full spectrum and its expanded region.

12. CD spectroscopy:

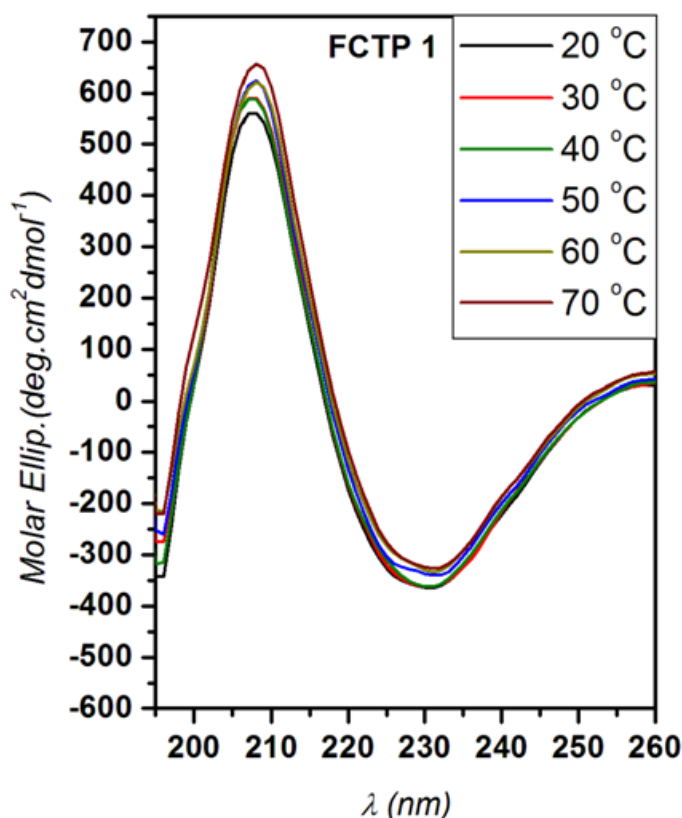


Figure S36: Temperature dependent CD spectra of FCTP **1** and in MeOH at 500 μM concentration over the range of 20 – 70 $^{\circ}\text{C}$.

13. Restrained Molecular Dynamics Calculations and Molecular Modeling:

The molecular dynamic studies were carried out on MacroModel with OPLS force field, version 10.3 program from Schrodinger software, using the NOESY restraints. For cyclic peptide **1** and **2** molecular dynamics calculation was carried out at 300 K in CDCl_3 (dielectric constant = 4.7) solvent. Duplicates were detected and eliminated using root-mean-squared difference (RMSD) of the torsion angles. These structures displayed low RMSD values ($\text{RMSD} < 0.3 \text{ \AA}$) on superimposition. Distance constraints used in MD calculations as well as molecular modeling for fluorinated cyclic tetrapeptide (FCTP) **1** and fluorinated cyclic hexapeptide (FCHP) **2** derived from NOESY experiment are given in Table S2 and S3, respectively.

The tetrameric self-assembly model of CPs **1** and **2** was constructed from the initially obtained monomeric structures from NMR-MD studies. These model assembly structures were prior optimized by molecular mechanics force field method (MMFF) and finely

subjected to semi-empirical PM6 method that resulted tubular self-assembly formation (Figure S37c-f). The self-assembled pores of **1** and **2** is roughly oval and triangular in shape, respectively, with internal van der Waals diameter of 5.7 Å between the Val- α -carbon for **1** and 9.7 Å between the Val- α -carbon sugar C4 carbon for **2**. All the calculations were performed by using *Spartan '14 software*.^[2S]

Table S2: Distance constraints used in MD calculations for FCTP **1** derived from NOESY experiment.

| (F2) [ppm] | (F1) [ppm] | Average Distances (Å) | | Between (F1/F2) |
|------------|------------|-----------------------|-------------|-----------------|
| | | Upper Bound | Lower Bound | |
| 4.2491 | 3.1462 | 1.98 | 1.62 | Ha-5/Hb-5 |
| 4.8369 | 3.1462 | 2.43 | 1.99 | Hb-5/H-4 |
| 6.8034 | 3.1503 | 2.93 | 2.39 | Hb-5/NH-1 |
| 7.2128 | 4.8491 | 4.28 | 3.5 | H-4/NH-2 |
| 7.2047 | 4.6464 | 3.03 | 2.48 | H-1/NH-2 |
| 7.2128 | 4.4923 | 2.89 | 2.37 | α H/NH-2 |
| 7.2169 | 4.2409 | 4.21 | 3.44 | Hb-5/NH-2 |
| 7.2088 | 1.9786 | 2.95 | 2.41 | β H/NH-2 |
| 7.2047 | 0.9163 | 2.74 | 2.24 | Me (Val)/NH-2 |
| 6.8034 | 0.9082 | 2.87 | 2.35 | Me (Val)/NH-1 |
| 6.7993 | 1.5042 | 3.7 | 3.03 | Me1 (ace)/NH-1 |
| 6.8115 | 4.245 | 3.37 | 2.76 | Hb-5/NH-1 |
| 6.8074 | 4.4964 | 2.31 | 1.89 | α H/NH-1 |
| 6.8034 | 4.8329 | 2.47 | 2.02 | 4H/NH-1 |
| 6.0249 | 1.3218 | 2.62 | 2.14 | Me-2 (ace)/H-1 |
| 6.0208 | 1.5083 | 3.77 | 3.09 | Me-1-(ace)/H-1 |
| 6.0249 | 3.1503 | 5.13 | 4.19 | Ha-5/H-1 |
| 6.029 | 4.2369 | 4.35 | 3.56 | Hb-5/H-1 |
| 6.0249 | 4.6464 | 2.2 | 1.8 | H-1/H-2 |
| 6.0249 | 4.8329 | 3.34 | 2.73 | H-4/H-1 |
| 6.8074 | 1.9745 | 3.2 | 2.62 | β H/NH-1 |
| 4.8369 | 1.5042 | 2.6 | 2.12 | Me-1 (ace)/H-4 |
| 4.6464 | 0.9244 | 3.18 | 2.6 | Me (Val)/H-2 |
| 4.6504 | 1.3218 | 2.63 | 2.15 | Me-2 (ace)/H-2 |

| | | | | |
|--------|--------|------|------|-----------------------|
| 4.6464 | 1.5083 | 4.19 | 3.43 | Me-1 (ace)/H-4 |
| 4.5004 | 0.9204 | 2.35 | 1.92 | Me (Val)/ α H |
| 4.4964 | 1.9745 | 2.42 | 1.98 | β H/ α H |
| 3.1503 | 0.9244 | 4.17 | 3.41 | Me (Val)/Ha-5 |
| 3.1462 | 1.5123 | 3.1 | 2.54 | Me-1 (ace)/Ha-5 |
| 1.9745 | 0.9163 | 1.97 | 1.61 | Me (Val)/ β H |
| 1.5123 | 1.3218 | 2.22 | 1.81 | Me-2 (ace)/Me-1 (ace) |
| 1.5083 | 0.9082 | 2.4 | 1.96 | Me-2 (ace)/Me (Val) |
| 7.2007 | 6.8074 | 4.45 | 3.64 | NH-2/NH-1 |

Table S3: Distance constraints used in MD calculations for FCHP2 derived from NOESY experiment.

| (F2) [ppm] | (F1) [ppm] | Average Distances (\AA) | | Between (F1/F2) |
|------------|------------|------------------------------------|-------------|------------------|
| | | Upper Bound | Lower Bound | |
| 3.9409 | 3.5436 | 1.98 | 1.62 | Ha-5/Hb-5 |
| 4.4761 | 3.5395 | 3.14 | 2.57 | Ha-5/ α H |
| 4.618 | 3.5355 | 2.79 | 2.28 | 5-Ha/H-4 |
| 7.0628 | 6.7506 | 3.21 | 2.63 | NH-1/NH-2 |
| 7.0669 | 4.6991 | 2.91 | 2.38 | NH-1/H-2 |
| 7.0628 | 4.5896 | 3.75 | 3.07 | NH-2/H-4 |
| 7.0669 | 4.468 | 2.92 | 2.39 | NH-2/ α H |
| 7.0628 | 2.2583 | 3.03 | 2.48 | NH-2/ β H |
| 7.0709 | 1.5853 | 4.12 | 3.37 | NH-2/Me-1(ace) |
| 7.0709 | 0.9244 | 2.49 | 2.04 | NH-2/Me (Val) |
| 6.7588 | 0.9163 | 3.06 | 2.5 | NH-1/Me (Val) |
| 6.7547 | 2.2624 | 2.91 | 2.38 | NH-1/ β H |
| 6.7588 | 3.5355 | 2.87 | 2.35 | NH-1/Ha-5 |
| 6.7547 | 3.9328 | 3.21 | 2.63 | NH-1/Hb-5 |
| 6.7547 | 4.468 | 2.42 | 1.98 | NH-1/ α H |
| 6.7506 | 4.6221 | 2.76 | 2.26 | NH-1/H-4 |
| 6.0168 | 1.3745 | 2.68 | 2.19 | H-1/Me-2 (ace) |
| 6.0208 | 1.5812 | 3.74 | 3.06 | H-1/Me-1 (ace) |
| 6.0168 | 3.5517 | 5.01 | 4.1 | H-1/Ha-5 |
| 6.0127 | 3.9328 | 4.63 | 3.79 | H-1/Hb-5 |
| 6.0127 | 4.7032 | 2.2 | 1.8 | H-1/H-2 |

| | | | | |
|--------|--------|------|------|-----------------------|
| 6.0168 | 4.5856 | 3.44 | 2.81 | H-1/H-4 |
| 4.7032 | 0.9366 | 3.62 | 2.97 | H-2/Me (Val) |
| 4.7072 | 1.3704 | 2.66 | 2.18 | H-2/Me2-can |
| 4.7032 | 1.5772 | 3.81 | 3.11 | H-2/Me-1 (ace) |
| 4.614 | 1.5893 | 2.55 | 2.09 | Me-1 (ace)/H-4 |
| 4.472 | 2.2624 | 2.32 | 1.9 | α H/ β H |
| 4.618 | 3.9369 | 2.61 | 2.13 | H-4/Hb-5 |
| 4.618 | 0.9204 | 2.96 | 2.42 | Me (Val)/H-4 |
| 4.472 | 0.9285 | 2.31 | 1.89 | Me (Val)/aH |
| 3.5517 | 0.9082 | 3.86 | 3.16 | Me (Val)/Ha-5 |
| 3.5395 | 2.2583 | 4.87 | 3.99 | Ha-5/ β H |
| 2.2705 | 0.9244 | 1.99 | 1.63 | Me (Val)/ β H |
| 1.5975 | 1.3623 | 2.32 | 1.9 | Me (Val)/Me-2 (ace) |
| 1.5975 | 0.9041 | 2.75 | 2.25 | Me-2 (ace)/Me-1 (ace) |

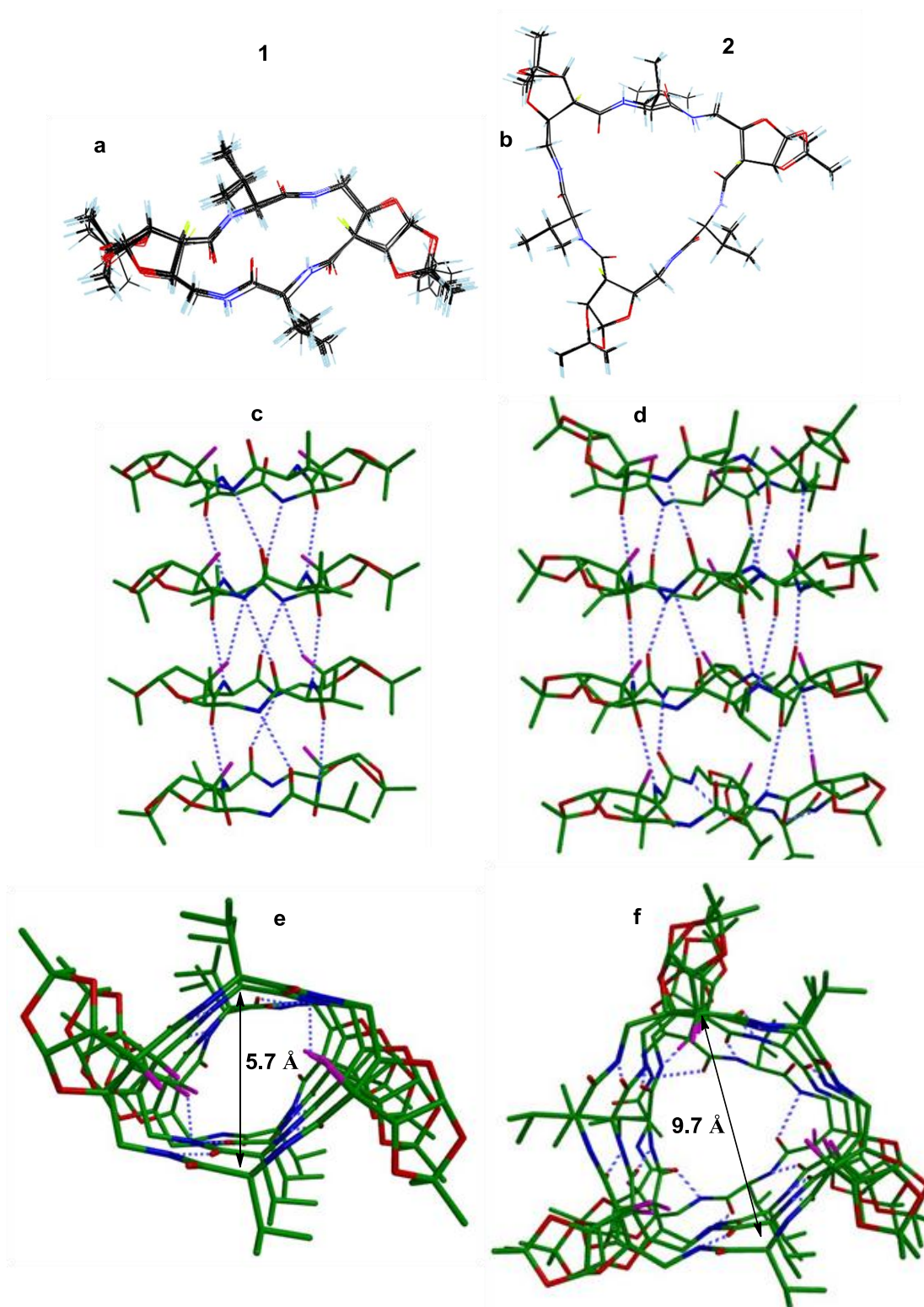


Figure S37: Superimposed energy minimized NMR-MD structures of FCTP 1 and FCHP 2 (a and b) and schematic side (c and d) and top (e and f) views of self-assembled tubular structures obtained by molecular modeling using PM6 method (colours codes for (a-b): Carbon = black, oxygen = red, nitrogen = blue, hydrogen = sky blue, fluorine = faint yellow; for (c-f) Carbon = green, oxygen = red, nitrogen = blue, , fluorine = pink. Hydrogen atoms are omitted for sake of clarity.

14. X-ray Crystallography (CCDC 1573315):

X-ray intensity data measurements of compound α,γ -cyclic tetrapeptide (FCTP) **1** was carried out on a Bruker D8 VENTURE Kappa Duo PHOTON II CPAD diffractometer equipped with Incoatech multilayer mirrors optics.^[3S] The intensity measurements were carried out with Cu micro-focus sealed tube diffraction source ($\text{CuK}\alpha = 1.54178 \text{ \AA}$) at 100(2) K temperature. The X-ray generator was operated at 50 kV and 1.1 mA. A preliminary set of cell constants and an orientation matrix were calculated from three sets of 40 frames. Data were collected with φ and ω shutter less scan width of 0.5° at different settings of ω , φ and 2θ with a frame time of 60 secs keeping the sample-to-detector distance fixed at 5.00 cm. The X-ray data collection was monitored by APEX3 program (Bruker, 2016).¹ All the data were corrected for Lorentzian, polarization and absorption effects using SAINT and SADABS programs (Bruker, 2016). ShelX-97 was used for structure solution and full matrix least-squares refinement on F^2 .² All the hydrogen atoms were placed in a geometrically idealized positions and constrained to ride on its parent atoms. An ORTEP III³ view of compound was drawn with 30% probability displacement ellipsoids and H atoms are shown as small spheres of arbitrary radii.

Crystal data of α,γ -cyclic tetrapeptide (FCTP) **1** (CCDC 1573315): $\text{C}_{28}\text{H}_{42}\text{F}_2\text{N}_4\text{O}_{10} \cdot 2.5(\text{H}_2\text{O})$, $M = 672.65$, colorless needle, $0.44 \times 0.32 \times 0.19 \text{ mm}^3$, monoclinic, chiral space group $P2_1$, $a = 14.578(2) \text{ \AA}$, $b = 13.1698(17) \text{ \AA}$, $c = 19.698(3) \text{ \AA}$, $\beta = 106.053(7)^\circ$, $V = 3634.4(8) \text{ \AA}^3$, $Z = 4$, $T = 100(2) \text{ K}$, $2\theta_{\text{max}} = 135^\circ$, $D_{\text{calc}} (\text{g cm}^{-3}) = 1.229$, $F(000) = 1424$, $\mu (\text{mm}^{-1}) = 0.884$, 26646 reflections collected, 11813 unique reflections ($R_{\text{int}} = 0.1669$), 7767 observed ($I > 2\sigma(I)$) reflections, multi-scan absorption correction, $T_{\text{min}} = 0.699$, $T_{\text{max}} = 0.849$, 956 refined parameters, number of restraints = 123, Good of Fit = $S = 1.491$, $R1 = 0.1345$, $wR2 = 0.3783$ (all data $R = 0.1728$, $wR2 = 0.4271$), maximum and minimum residual electron densities; $\Delta\rho_{\text{max}} = 0.675$, $\Delta\rho_{\text{min}} = -0.384 (\text{e}\text{\AA}^{-3})$.

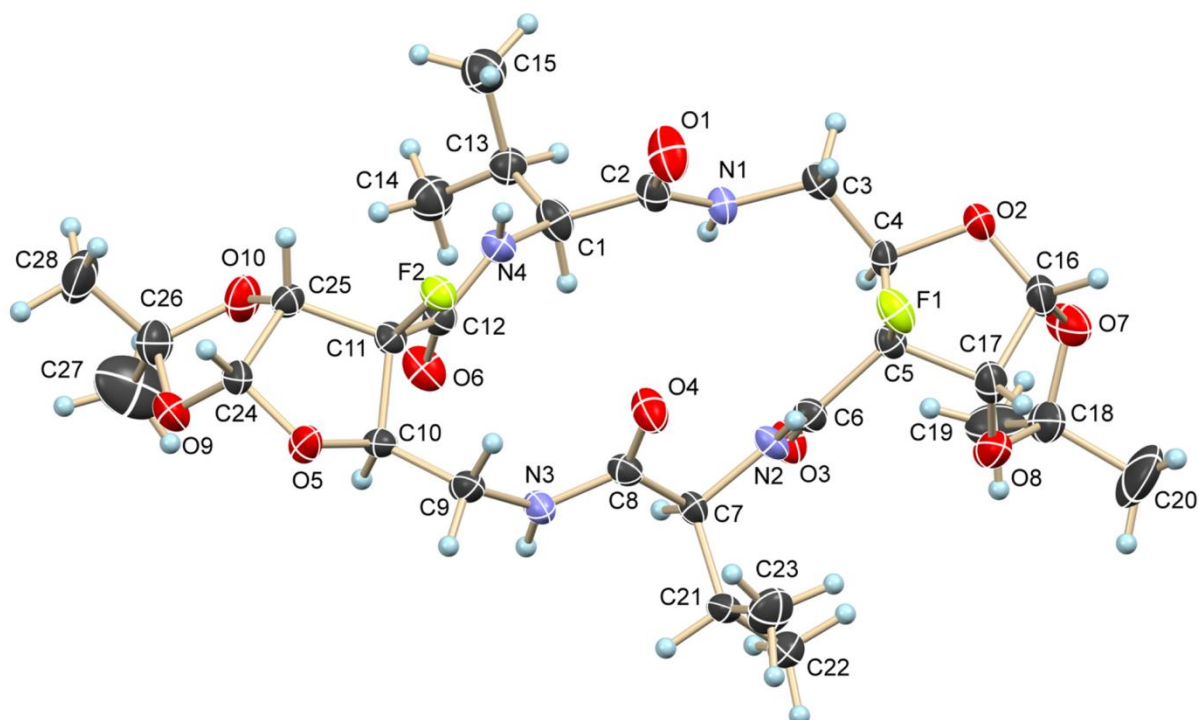


Figure S38: ORTEP diagram of FCTP **1** indicating flat oval-ring shaped β -strand conformation (Solvent molecules omitted for clarity)

Table S4: Calculated torsion angles from crystal structure of **1**.

| Residue | Angles | | | |
|---------|---------|---------|------------|------------|
| | ϕ | ψ | θ_1 | θ_2 |
| Sugar | 134.88 | -132.09 | -77.31 | 80.38 |
| Val | -139.37 | 151.7 | - | - |

15. Ion transport experiments:

A. Ion transporting activity studies across EYPC-LUV \supset HPTS:

Buffer and stock solution preparation: HEPES buffer was prepared by dissolving solid HEPES (10 mM) and NaCl (100 mM) in Milli-Q water, followed by adjustment of pH (pH = 7.0) by addition of 0.5 M NaOH solution. Stock solutions of all cyclic peptide (CP) derivatives were prepared in HPLC grade DMSO.

Preparation of EYPC-LUVs \supset HPTS: In a clean and dry small round bottom flask, 1 mL of egg yolk phosphatidylcholine (EYPC, 25 mg/mL in CHCl_3) was dried by purging nitrogen gas with continuous rotation to form a thin transparent film of EYPC. The transparent film was kept in high vacuum for 8 h to remove all trace of CHCl_3 at room temperature. The

resulting film was hydrated with 1 mL buffer (1 mM HPTS, 10 mM HEPES, 100 mM NaCl, pH = 7.0) for 1 h with 4-5 times occasional vortexing and subjected to freeze-thaw cycle (≥ 12 times). Extrusions were done 19 times (must be an odd number) by a Mini-extruder, equipped with a polycarbonate membrane of pore size 100 nm (or 200 nm), obtained from Avanti Polar Lipids. Extravesicular dyes were removed by gel filtration (using Sephadex G-50) with buffer (10 mM HEPES, 100 mM NaCl, pH = 7.0) and diluted to 6 mL to get EYPC-LUVs \Rightarrow HPTS: ~ 5.0 mM EYPC; inside: 1 mM HPTS, 10 mM HEPES, 100 mM NaCl, pH = 7.0, outside: 10 mM HEPES, 100 mM NaCl, pH = 7.0.^[45]

Ion transport activity: In a clean and dry fluorescence cuvette, 1975 μ L of HEPES buffer (10 mM HEPES, 100 mM NaCl, pH = 7.0) was added followed by addition of 25 μ L of EYPC-LUVs \Rightarrow HPTS. The cuvette was placed in the fluorescence instrument with slow stirring condition by a magnetic stirrer equipped in the instrument (at $t = 0$ s). The time course of HPTS fluorescence emission intensity, F_t was observed at $\lambda_{em} = 510$ nm ($\lambda_{ex} = 450$ nm). 20 μ L of 0.5 M NaOH was added to the cuvette at $t = 25$ s to create the pH gradient of ~ 0.8 between the extra and intra vesicular system. CP derivatives of different concentrations were added at $t = 100$ s, and finally 25 μ L of 10% Triton X-100 was added at $t = 300$ s to lyse vesicles resulting destruction of the pH gradient (Figure S39).

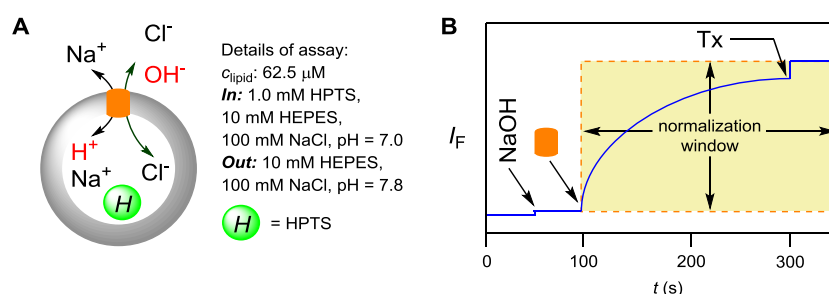


Figure S39: Representations of fluorescence based ion transport activity assay using EYPC-LUVs \Rightarrow HPTS (A), and illustration of ion transport kinetics showing normalization window (B).

For data analysis and comparison, time (X-axis) was normalized between the point of transporter addition (*i.e.* $t = 100$ s was normalized to $t = 0$ s) and end point of experiment (*i.e.* $t = 350$ s was normalized to $t = 250$ s).

Fluorescence intensities (F_t) were normalized to fractional emission intensity I_F using Equation S1:

$$I_F = [(F_t - F_0) / (F_\infty - F_0)] \times 100 \quad \text{Equation S1}$$

where, F_0 = Fluorescence intensity just before the channel forming molecule addition (at 0 s). F_∞ = Fluorescence intensity at saturation after complete leakage (at 320 s). F_t = Fluorescence intensity at time t .

The concentration profile data were analyzed by Hill equation (Equation S2) to get the Effective concentration (EC_{50}):

$$Y = Y_\infty + (Y_0 - Y_\infty) / [1 + (c/EC_{50})^n] \quad \text{Equation S2}$$

where, Y_0 = Fluorescence intensity just before the CP derivative addition (at $t = 0$ s), Y_∞ = Fluorescence intensity with excess compound concentration, c = Concentration of channel forming compound.

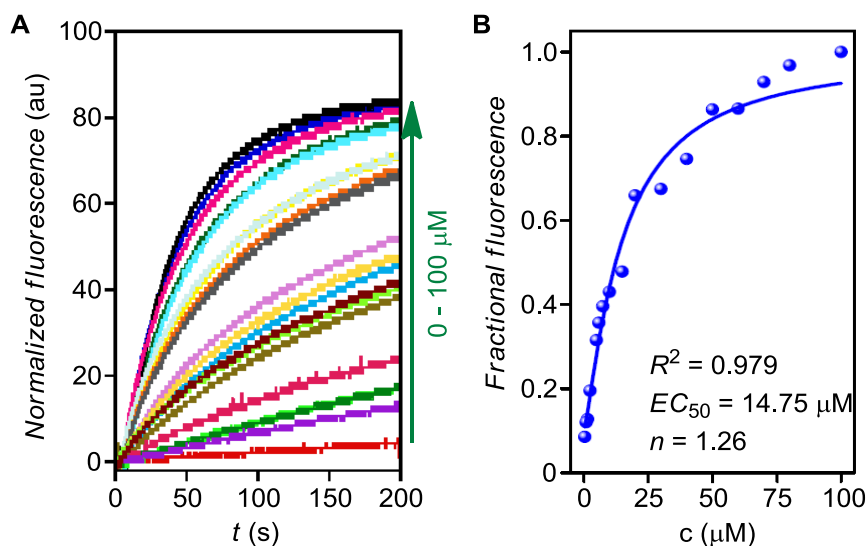


Figure S40: Concentration dependent ion transport activity of **1** (0–20 μM) across EYPC-LUVs⊃HPTS (A). Dose response plot of **1** and Hill analysis under the identical condition. The normalized fluorescence intensities at 100 s were used to generate the dose response plot (B).

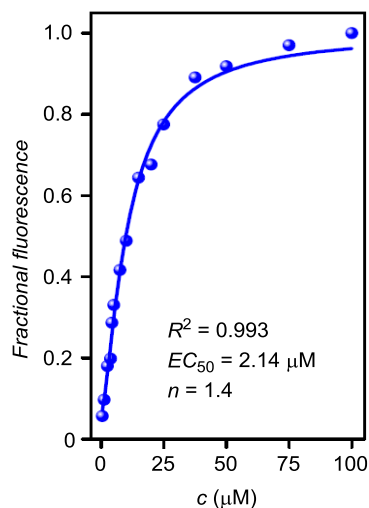


Figure S41: Dose response plot of **2** and Hill analysis in the identical condition. The normalized fluorescence intensities at 100 s were used to generate the dose response plot (**B**).

B. Ion selectivity studies across EYPC-LUVs \supset HPTS:

Buffer and stock solution preparation: HEPES buffer was prepared by dissolving appropriate amount of solid HEPES and a salt (either of NaCl, NaF, NaBr, NaI, NaNO₃, NaClO₄, LiCl, KCl, RbCl, and CsCl) in autoclaved milli-Qwater to get 10 mM HEPES and 100 mM salt, respectively. Subsequently, the pH was adjusted to 7.0 by addition of NaOH solution.

Preparation of EYPC-LUVs \supset HPTS: Vesicles were prepared in the same way as stated above.

Anion selectivity assay: In a clean and dry fluorescence cuvette, 1975 μL of HEPES buffer (10 mM HEPES, 100 mM NaA, pH = 7.0; where, A⁻ = F⁻, Cl⁻, Br⁻, I⁻, NO₃⁻, and ClO₄⁻) was added followed by addition of 25 μL of EYPC-LUVs \supset HPTS in slowly stirring condition by a magnetic stirrer equipped with the fluorescence instrument (at $t = 0$ s). The HPTS fluorescence emission intensity, F_t was observed at $\lambda_{\text{em}} = 510$ nm ($\lambda_{\text{ex}} = 450$ nm) with time. 20 μL of 0.5 M NaOH was added to the cuvette at $t = 25$ s to create the pH gradient ($\Delta\text{pH} \sim 0.8$) between the intra and extra vesicular system. CP derivatives were added at $t = 100$ s and of 10% Triton X-100 (25 μL) was added at $t = 300$ s to lyze vesicles for complete destruction of pH gradient (Figure S42A).

Cation selectivity assay: In a clean and dry fluorescence cuvette, 1975 μL of HEPES buffer (10 mM HEPES, 100 mM MCl, pH = 7.0; where, M⁺ = Li⁺, Na⁺, K⁺, Rb⁺ and Cs⁺) was added

followed by addition of 25 μL of EYPC-LUVs \supset HPTS in slowly stirring condition by a magnetic stirrer equipped with the fluorescence instrument (at $t = 0$ s). The HPTS fluorescence emission intensity, F_t was observed at $\lambda_{\text{em}} = 510$ nm ($\lambda_{\text{ex}} = 450$ nm) with time. 20 μL of 0.5 M NaOH was added to the cuvette at $t = 25$ s to create the pH gradient ($\Delta\text{pH} = 0.8$) between the intra and extra vesicular system. CP derivatives were added at $t = 100$ s and 10% Triton X-100 (25 μL) was added at $t = 300$ s to lyze vesicles for complete destruction of the pH gradient (Figure S42B).

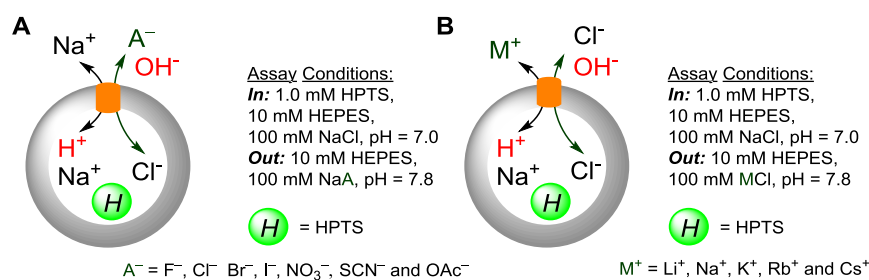


Figure S42: Schematic representations of the fluorescence based anion (**A**) and cation (**B**) selectivity assays.

For data analysis and comparison, time (X-axis) was normalized between the point of compound addition (*i.e.* $t = 100$ s was normalized to $t = 0$ s) and end point of experiment (*i.e.* $t = 350$ s was normalized to $t = 250$ s).

Fluorescence intensities (F_t) were normalized to fractional emission intensity I_F using Equation S1.

16. Anion recognition by ^1H NMR titration:

^1H NMR titrations were carried out in Bruker 500 MHz spectrometer at room temperature and calibrated to the residual solvent peak in CDCl_3 ($\delta = 7.26$ ppm). Titrations were performed by the addition of aliquots of tetrabutylammonium nitrate (TBANO_3) (30 mM CDCl_3) to the solution of receptor (~ 3 mM) CDCl_3 . Both TBA-salt and receptor were dried under high vacuum prior to use. All NMR data were processed in MestReNova 6 software and the change in chemical shift were plotted and that indicated no significant change in amide NHs or proton chemical shift (Figure S43).

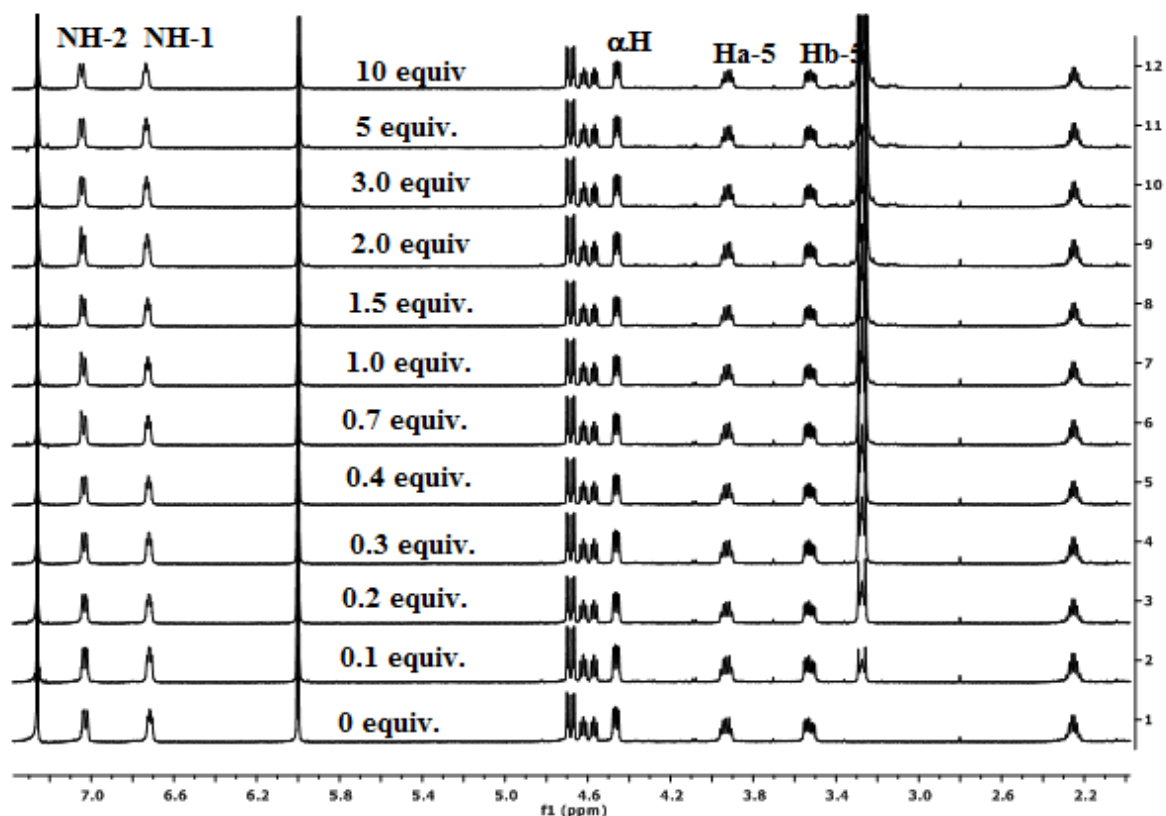


Figure S43: ^1H NMR titration spectra for **2** with stepwise addition of TBANO_3 in CDCl_3 solution on 500 MHz.

17. Anion recognition by ESI-MS spectroscopy:

Stock solutions of **2** and TBANO_3 (5 mM each) were prepared in spectroscopy grade CH_3CN . Solutions were mixed in equal proportion and diluted to get 5 μM concentrations of each species in CH_3CN and injected and spectra were recorded up to the range of 3500 Da. The ESI-MS data recorded from CH_3CN solution of **2** with TBANO_3 prepared in 1:1 molar ratio.

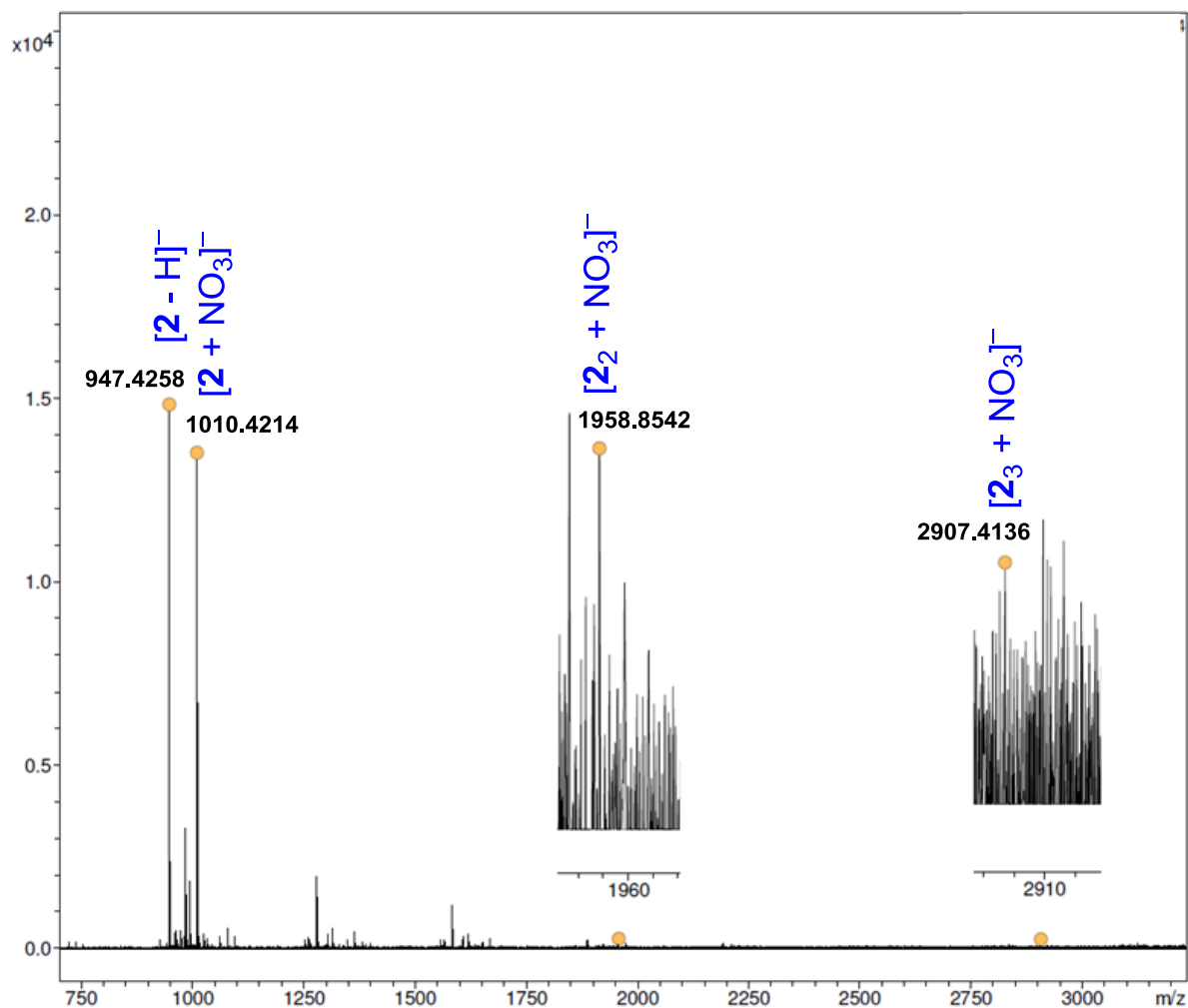


Figure S44: Expanded region of the ESI-MS spectrum that confirms the anion recognition by the supramolecular self-assembly of **2**.

18. Computational Methodology:

Optimization of $[2 + \text{NO}_3^-]$ complex:

The quantum chemical semi-empirical (PM6) and DFT calculations have been performed to obtain the complex of cyclic hexa-peptide **2** with Nitrate ion $[2 + \text{NO}_3^-]$. Initially nine different conformational geometries were generated randomly by placing NO_3^- ion on top or bottom to the cavity of the initially optimized structure of **2** from NMR and MD studies. The conformational geometries of $[2 + \text{NO}_3^-]$ complexes were initially optimized by semi-empirical PM6 method. The lowest energy conformation (obtained from PM6 modeling) of $[2 + \text{NO}_3^-]$ was subjected for automated full geometry optimization calculations by *ab-initio* Density Functional Theory (DFT) method by employing B3LYP/6-31G** basis set function. All calculations were performed by using *Spartan'14* (Wavefunction, inc.) molecular

modeling software. Therefore, the most stable conformation was considered as the final optimized structure of the $[2 + \text{NO}_3^-]$ complex in the gas phase (Figure S45).

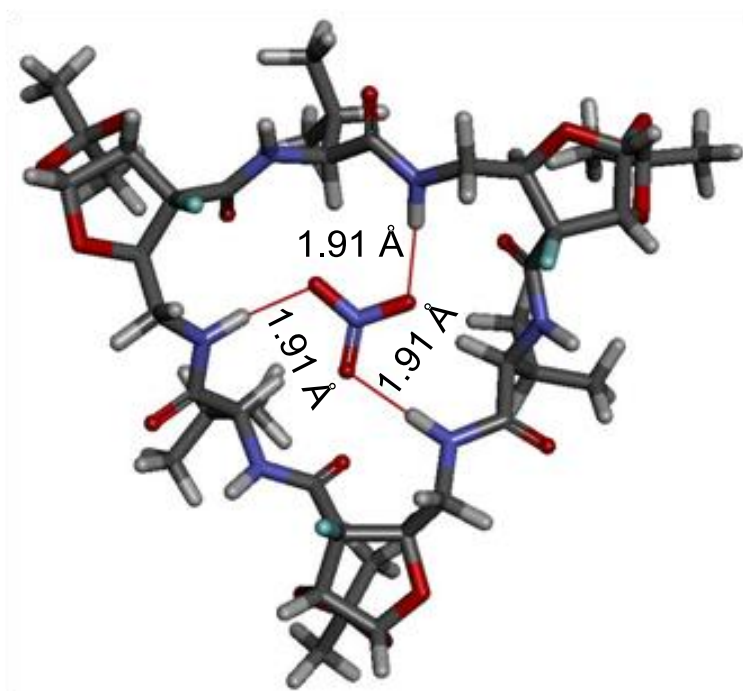


Figure S45: Geometry optimized structure of $[2 + \text{NO}_3^-]$ complex by DFT calculation.

Table S5: Atomic co-ordinates of the optimized structure of lowest energy conformation (Figure S45) obtained for $[2 + \text{NO}_3^-]$ from DFT B3LYP/6-311G** geometry optimization.

Total Energy = -3675.413 au

| Atom no. | Atom Type | x | y | z |
|----------|-----------|--------|-------|--------|
| 1 | O | -1.683 | 6.339 | -0.715 |
| 2 | C | -1.471 | 4.984 | -0.261 |
| 3 | C | -2.883 | 4.521 | 0.134 |
| 4 | C | -3.578 | 5.822 | 0.628 |
| 5 | C | -2.606 | 6.929 | 0.144 |
| 6 | O | -1.999 | 7.379 | 1.349 |
| 7 | C | -2.762 | 6.974 | 2.485 |
| 8 | O | -3.686 | 5.971 | 2.019 |
| 9 | C | -1.834 | 6.364 | 3.526 |
| 10 | C | -3.57 | 8.158 | 3.017 |
| 11 | C | -0.766 | 4.166 | -1.353 |
| 12 | N | 0.406 | 3.472 | -0.84 |
| 13 | C | 1.598 | 3.553 | -1.478 |
| 14 | C | 2.765 | 2.842 | -0.776 |
| 15 | N | 3.51 | 2.162 | -1.837 |

| | | | | |
|----|---|--------|--------|--------|
| 16 | C | 3.599 | 3.876 | 0.042 |
| 17 | C | 4.527 | 3.183 | 1.051 |
| 18 | C | 4.377 | 4.852 | -0.85 |
| 19 | C | 4.106 | 0.963 | -1.68 |
| 20 | C | 4.429 | 0.234 | -2.99 |
| 21 | C | 5.898 | 0.345 | -3.491 |
| 22 | C | 6.222 | -1.109 | -3.92 |
| 23 | O | 5.029 | -1.824 | -3.929 |
| 24 | C | 4.183 | -1.282 | -2.89 |
| 25 | O | 7.104 | -1.559 | -2.899 |
| 26 | C | 7.661 | -0.454 | -2.19 |
| 27 | O | 6.853 | 0.693 | -2.522 |
| 28 | C | 7.571 | -0.722 | -0.695 |
| 29 | C | 9.088 | -0.19 | -2.674 |
| 30 | C | 2.74 | -1.756 | -3.107 |
| 31 | N | 2.136 | -2.277 | -1.888 |
| 32 | C | 1.462 | -3.451 | -1.908 |
| 33 | C | 0.888 | -3.914 | -0.56 |
| 34 | N | -0.447 | -4.431 | -0.869 |
| 35 | C | 1.846 | -4.949 | 0.106 |
| 36 | C | 1.519 | -5.143 | 1.594 |
| 37 | C | 1.879 | -6.289 | -0.639 |
| 38 | C | -1.515 | -4.302 | -0.055 |
| 39 | C | -3.582 | -5.835 | -0.592 |
| 40 | C | -5.059 | -5.421 | -0.36 |
| 41 | O | -5.165 | -4.057 | -0.621 |
| 42 | C | -3.907 | -3.445 | -0.26 |
| 43 | C | -2.868 | -4.464 | -0.759 |
| 44 | C | -3.819 | -2.034 | -0.859 |
| 45 | N | -3.413 | -1.044 | 0.127 |
| 46 | O | -5.27 | -5.718 | 1.015 |
| 47 | C | -4.248 | -6.577 | 1.517 |
| 48 | O | -3.203 | -6.594 | 0.526 |
| 49 | C | -3.703 | -6.007 | 2.821 |
| 50 | C | -4.791 | -7.999 | 1.664 |
| 51 | C | -4.131 | 0.09 | 0.307 |
| 52 | C | -3.626 | 1.021 | 1.421 |
| 53 | N | -3.746 | 2.377 | 0.883 |
| 54 | C | -2.844 | 3.35 | 1.123 |
| 55 | C | -4.428 | 0.774 | 2.735 |
| 56 | C | -3.734 | 1.414 | 3.946 |
| 57 | C | -5.891 | 1.224 | 2.633 |
| 58 | H | 6.681 | -1.23 | -4.907 |
| 59 | H | 4.542 | -1.614 | -1.912 |
| 60 | H | -3.424 | -6.411 | -1.509 |
| 61 | H | -5.806 | -5.929 | -0.978 |

| | | | | |
|-----|---|--------|--------|--------|
| 62 | H | -3.823 | -3.386 | 0.828 |
| 63 | H | 2.135 | -0.943 | -3.52 |
| 64 | H | 2.746 | -2.568 | -3.835 |
| 65 | H | 1.92 | -1.603 | -1.146 |
| 66 | H | 0.761 | -3.058 | 0.11 |
| 67 | H | -0.615 | -4.596 | -1.854 |
| 68 | H | 2.845 | -4.494 | 0.043 |
| 69 | H | 2.246 | -5.824 | 2.052 |
| 70 | H | 1.551 | -4.194 | 2.137 |
| 71 | H | 0.518 | -5.559 | 1.733 |
| 72 | H | 0.905 | -6.787 | -0.575 |
| 73 | H | 2.117 | -6.153 | -1.697 |
| 74 | H | 2.625 | -6.954 | -0.191 |
| 75 | H | -3.133 | -2.03 | -1.711 |
| 76 | H | -4.807 | -1.745 | -1.221 |
| 77 | H | -2.433 | -1.056 | 0.427 |
| 78 | H | -3.2 | -5.058 | 2.627 |
| 79 | H | -4.519 | -5.861 | 3.534 |
| 80 | H | -2.976 | -6.699 | 3.256 |
| 81 | H | -3.995 | -8.676 | 1.984 |
| 82 | H | -5.596 | -8.023 | 2.405 |
| 83 | H | -5.186 | -8.352 | 0.707 |
| 84 | F | 3.643 | 0.76 | -4.038 |
| 85 | F | -2.709 | -4.303 | -2.152 |
| 86 | F | -3.586 | 4.148 | -1.031 |
| 87 | O | -2.015 | 3.352 | 2.031 |
| 88 | O | -5.153 | 0.373 | -0.327 |
| 89 | O | -1.481 | -4.054 | 1.148 |
| 90 | O | 4.387 | 0.436 | -0.605 |
| 91 | O | 1.787 | 4.186 | -2.522 |
| 92 | O | 1.329 | -4.156 | -2.915 |
| 93 | H | -0.861 | 4.99 | 0.646 |
| 94 | H | -2.407 | 6.086 | 4.415 |
| 95 | H | -1.369 | 5.463 | 3.123 |
| 96 | H | -3.697 | 2.502 | 3.855 |
| 97 | H | -4.276 | 1.163 | 4.866 |
| 98 | H | -5.949 | 2.315 | 2.541 |
| 99 | H | -6.442 | 0.935 | 3.535 |
| 100 | H | -6.386 | 0.787 | 1.763 |
| 101 | H | -4.41 | -0.316 | 2.878 |
| 102 | H | -2.703 | 1.062 | 4.05 |
| 103 | H | -4.339 | 2.459 | 0.066 |
| 104 | H | -2.566 | 0.839 | 1.613 |
| 105 | H | 2.385 | 2.072 | -0.099 |
| 106 | H | 5.916 | 1.065 | -4.315 |
| 107 | H | 6.523 | -0.774 | -0.394 |

| | | | | |
|-----|---|--------|--------|--------|
| 108 | H | 8.079 | -1.66 | -0.454 |
| 109 | H | 8.05 | 0.09 | -0.139 |
| 110 | H | 9.729 | -1.048 | -2.449 |
| 111 | H | 9.095 | -0.023 | -3.754 |
| 112 | H | 9.498 | 0.696 | -2.182 |
| 113 | H | 3.282 | 2.465 | -2.777 |
| 114 | H | 4.861 | 5.621 | -0.237 |
| 115 | H | 3.723 | 5.339 | -1.576 |
| 116 | H | 5.162 | 4.324 | -1.404 |
| 117 | H | 2.855 | 4.45 | 0.613 |
| 118 | H | 5.256 | 2.545 | 0.546 |
| 119 | H | 3.962 | 2.546 | 1.739 |
| 120 | H | 5.067 | 3.933 | 1.641 |
| 121 | H | 0.243 | 2.675 | -0.216 |
| 122 | H | -0.427 | 4.843 | -2.138 |
| 123 | H | -1.468 | 3.456 | -1.802 |
| 124 | H | -4.569 | 5.868 | 0.167 |
| 125 | H | -3.059 | 7.768 | -0.394 |
| 126 | H | -1.067 | 7.088 | 3.815 |
| 127 | H | -2.899 | 8.952 | 3.358 |
| 128 | H | -4.197 | 7.843 | 3.856 |
| 129 | H | -4.216 | 8.558 | 2.231 |
| 130 | N | 0.043 | -0.026 | 0.072 |
| 131 | O | -0.528 | -1.139 | 0.225 |
| 132 | O | -0.564 | 1.037 | 0.369 |
| 133 | O | 1.222 | 0.023 | -0.371 |

19. References:

- (1S) Burade, S. S.; Shinde, S. V.; Bhuma, N.; Kumbhar, N.; Kotmale, A.; Rajamohanan, P. R.; Gonnade, R. G.; Talukdar, P.; Dhavale, D. D.; *J. Org.Chem.* **2017**, *82*, 5826.
- (2S) (a) Francl, M. M.; Pietro, W. J.; Hehre, W. J.; Binkley, J. S.; Gordon, M. S.; DeFrees, D. J.; Pople, J. A. *J. Chem. Phys.* **1982**, *77*, 3654. (b) Shao, Y.; Molnar, L. F.; Jung, Y.; Kussmann, J.; Ochsenfeld, C.; Brown, S. T.; Gilbert, A. T. B.; Slipchenko, L. V.; Levchenko, S. V.; O'Neill, D. P.; DiStasio, R. A., Jr.; Lochan, R. C.; Wang, T.; Beran, G. J. O.; Besley, N. A.; Herbert, J. M.; Lin, C. Y.; Van Voorhis, T.; Chien, S. H.; Sodt, A.; Steele, R. P.; Rassolov, V. A.; Maslen, P. E.; Korambath, P. P.; Adamson, R. D.; Austin, B.; Baker, J.; Byrd, E. F. C.; Dachsel, H.; Doerksen, R. J.; Dreuw, A.; Dunietz, B. D.; Dutoi, A. D.; Furlani, T. R.; Gwaltney, S. R.; Heyden, A.; Hirata, S.; Hsu, C.-P.; Kedziora, G.; Khalliulin, R. Z.; Klunzinger, P.; Lee, A. M.; Lee, M. S.; Liang, W.; Lotan, I.; Nair, N.; Peters, B.; Proynov, E. I.; Pieniazek, P. A.; Rhee, Y. M.; Ritchie, J.; Rosta, E.; Sherrill, C. D.; Simmonett, A. C.; Subotnik, J. E.; Woodcock, H. L., III; Zhang, W.; Bell, A. T.; Chakraborty, A. K.; Chipman, D. M.; Keil, F. J.; Warshel, A.; Hehre, W. J.; Schaefer, H. F., III; Kong, J.; Krylov, A. I.; Gill, P. M. W.; Head-Gordon, M. *Phys. Chem. Chem. Phys.* **2006**, *8*, 3172.
- (3S) a) Bruker (2016). *APEX2, SAINT and SADABS*. Bruker AXS Inc., Madison, Wisconsin, USA. (b) Sheldrick, G. M. *Acta Crystallogr.*, **2008**, *A64*, 112. (c) Farrugia, L. J. *J. Appl. Cryst.* **1997**, *30*, 565.
- (4S) (a) Saha, T.; Dasari, S.; Tewari, D.; Prathap, A.; Sureshan, K. M.; Bera, A. K.; Mukherjee, A.; Talukdar, P.; *J. Am. Chem. Soc.* **2014**, *136*, 14128. (b) Shinde, S. V.; Talukdar, P. *Angew. Chem. Int. Ed.* **2017**, *56*, 4238.